npj | Materials Degradation

www.nature.com/npjmatdeg

REVIEW ARTICLE OPEN

Corrosion of high entropy alloys

Yao Qiu[1], Sebastian Thomas[1], Mark A. Gibson[1,2], Hamish L. Fraser[1,3] and Nick Birbilis[1]

High entropy alloys represent a unique class of metal alloys, comprising nominally five or more elements in near equiatomic proportions. High entropy alloys have gained significant interest on the basis that the high configurational entropy of such alloy systems is purported to result in a single-phase solid solution structure. While such a single-phase structure can occur in unique systems, it is now appreciated that the definition of high entropy alloys can be broader, with systems comprising only four elements possible of forming single phases, and most five (or more) element systems actually being multi (>2) phases. To this end, the notion of compositionally complex alloys is a more general description, with the concise review herein focusing on the corrosion of compositionally complex alloys (inclusive of high entropy alloys). It is noted that generally, in spite of complex compositions and in many cases complicated microstructural heterogeneity, compositionally complex alloys are nominally corrosion-resistant. This is discussed and aspects of the status and needs are presented.

npj Materials Degradation (2017)1:15 ; doi:10.1038/s41529-017-0009-y

INTRODUCTION

High entropy alloys (HEAs) are systems that comprise five (but possibly more) principal metallic elements in near equiatomic ratios, forming one or more solid solution phases.[1] These alloys are termed HEAs because they have a high entropy of mixing compared to conventional alloys, thus notionally favouring the formation of solid solution phases. Such alloys were first synthesised about a decade ago by Cantor et al.,[2] wherein a five component $Fe_{20}Cr_{20}Mn_{20}Ni_{20}Co_{20}$ alloy was manufactured by melt spinning. The five transition metal elements used to manufacture that HEA were found to exhibit a high degree of intersolubility to form a single FCC solid solution. In the same period, Yeh et al.[1, 3] reported several HEAs produced by arc melting, comprising a number of elements including Cu, Ti, Cr, Ni, Co, Cr, V, Fe and Al. Continued research has however highlighted that numerous so-called HEAs, such as the $Mo_{0.5}AlNbTa_{0.5}TiZr$ system, did not have high configurational entropies and present the formation of secondary phases (rather than just solid solution phases). Therefore, a more general description of such alloy systems has emerged, with the more general naming and definition being compositionally complex alloys (CCAs),[4, 5] which is the preferred naming used throughout this review.

CCAs possess several unique and attractive properties, making them prime candidates for a number of engineering applications, such as applications that require high hardness,[6, 7] damage tolerance,[8–10] high thermal stability,[11, 12] and good wear resistance.[12] Some CCAs are now appreciated to possess a simple FCC and/or BCC microstructure,[10, 13, 14] such as the $Al_{0.3}CoCrFeNi$ system, which has a single FCC solution phase (Fig. 1a). Other CCAs, however, have more complex and heterogeneous microstructures[6, 15, 16] such as the $Mo_{0.5}AlNbTa_{0.5}TiZr$ system, which has a BCC + B2 microstructure (Fig. 1b). In another example, it has been shown that not only are CCA microstructures unique, but the extensive segregation of alloying elements can occur.[5] This extensive segregation of alloying elements is shown in Fig. 1b for the $AlMo_{0.5}NbTa_{0.5}TiZr$ system.

It is evident from Fig. 1b that significant gradients in local chemistry can exist in CCAs. How such alloys therefore behave in terms of their corrosion characteristics merits critical investigation. The microstructures that may evolve in CCAs, and the accompanying elemental segregation is unlike that seen in most other engineering alloys, and the influence of such microstructures on passivity (and uniformity of dissolution and/or surface films) is largely unknown. According to the literature published to date, the corrosion characteristics of select CCAs (and therein, HEAs) are reviewed and discussed in this study. Herein, specifically the influence of alloying elements such as aluminium, titanium, chromium, molybdenum and nickel on corrosion of CCAs are examined. Also, the impact of different processing methods such as anodisation and aging on the corrosion characteristics of the resultant CCAs are also briefly described.

AQUEOUS CORROSION OF HEAS

Chen et al.[17] conducted one of the earliest lines of work on the corrosion characteristics of HEAs. They investigated the corrosion of the $Cu_{0.5}NiAlCoCrFeSi$ alloy in H_2SO_4 and NaCl solutions and compared it with the corrosion characteristics of an austenitic stainless steel (AISI 304 SS). The concentrations of the solutions were varied from 0.1 to 1 M, and it was observed that the $Cu_{0.5}NiAlCoCrFeSi$ alloy had a lower corrosion rate (as defined by the corrosion current density, i_{corr}) than 304SS in all the test solutions. However, the pitting potential (E_{pit}) of $Cu_{0.5}NiAlCoCrFeSi$ was found to be lower (less noble) than that of 304SS in a Cl^- environment, and it was thus purported that the HEA had lower resistance to pitting than 304 SS.[17] The study however did not outline any of the mechanistic aspects pertaining to the corrosion of HEAs, while it is now also more widely appreciated in the corrosion community that the pitting potential is not the best

[1]Department of Materials Science and Engineering, Monash University, Clayton, VIC 3800, Australia; [2]CSIRO Manufacturing, Clayton, VIC 3168, Australia and [3]Department of Materials Science and Engineering, The Ohio State University, Columbus, OH 43210, USA
Correspondence: Nick Birbilis (nick.birbilis@monash.edu)

Received: 26 January 2017 Revised: 12 June 2017 Accepted: 3 July 2017
Published online: 21 August 2017

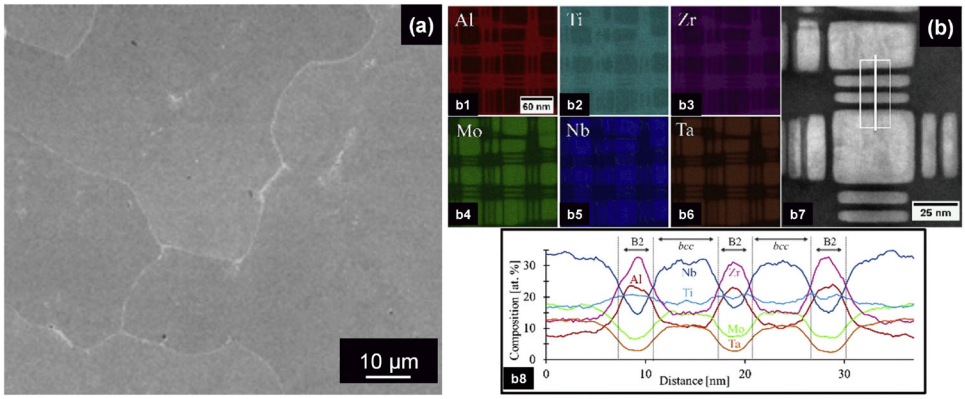

Fig. 1 **a** SEM micrograph of an as-cast $Al_{0.3}CoCrFeNi$ showing a single phase microstructure,[14] **b** (b1–b6) XEDS elemental maps of Al, Ti, Zr, Mo, Nb and Ta, respectively, recorded in STEM using the Super-X™ detector, (b7) A STEM-HAADF image with a white line identifying the location of the EDXS linescan shown in (b8).[5] (**a** reprinted with permission from ref. 14 with permission from Elsevier; **b** reprinted from ref. 5 with permission from Elsevier)

indication of pitting susceptibility, offering little insight into the number and size of pits that evolve. Recently, Qiu et al.[18] measured the E_{corr} (corrosion potential) and E_{pit} values for about 20 unique HEAs in 0.6 M NaCl and also reported a preliminary galvanic series for HEAs. Overall, HEAs were all determined to be significantly nobler than carbon steels and aluminium alloys. The E_{corr} values of the HEAs reported were nominally in the range of ferritic and austenitic stainless steels, with some HEAs (such as those containing the combination of Co, Cr and Ni) being even more noble than austenitic stainless steel. The E_{corr}, E_{pit} and i_{corr} of the HEAs primarily depended upon the respective alloying elements used to synthesise the HEA.[18] As a result, the effect of the different alloying elements on the corrosion of HEAs is presented herein, with some unifying tabulations and a galvanic series compiled further below.

The influence of different alloying elements on the corrosion of CCAs

The influence of aluminium on the corrosion of CCAs. Aluminium (Al) is a light metal and may therefore be used to lower the density of CCAs. It has also been reported that Al serves to increase the mechanical strength of the HEAs.[6, 19–24] Al/Al alloys are lower in the galvanic series (i.e., less noble) compared to the other elements that are used to synthesise HEAs namely Fe, Ni, Cr, Co and Ti.[25] Therefore, it is plausible that Al atoms may be preferentially released from a solid solution containing more noble elements during exposure to aqueous environments, in processes akin to dealloying. The corrosion rate of CCAs with Al may therefore be expected to increase with increasing Al content in depassivating conditions or conditions that promote dissolution; however, the beneficial role of Al when incorporated into surface films for passive alloys (in passive conditions) is well documented in the case of Ni-based corrosion-resistant alloys (CRAs).[26]

The influence of the Al concentration on the corrosion of $Al_xCrFe_{1.5}MnNi_{0.5}$ alloys in H_2SO_4 + NaCl solutions was investigated by Lee et al.[27] In such alloy notations, '*x*' defines the molar ratio of Al in the alloy and was taken as 0, 0.3 and 0.5 mol of Al, respectively. It was observed that an increase in the Al content increased the corrosion current density (i_{corr}) values of this HEA in 0.5 M H_2SO_4 (Fig. 2a), although the effect was only rather subtle and not considered outside the range of scatter of potentiodynamic polarisation testing. The $Al_xCrFe_{1.5}MnNi_{0.5}$ alloys displayed a clear window of passivity, with a polarisation response typical of stainless steels. What was however of interest is that the Al^{-}-containing alloys exhibited distinct peaks at potentials between 0.25 and 0.5 V vs (SHE; Fig. 2a); however, the electrochemical processes pertaining to these peaks were not clarified in that

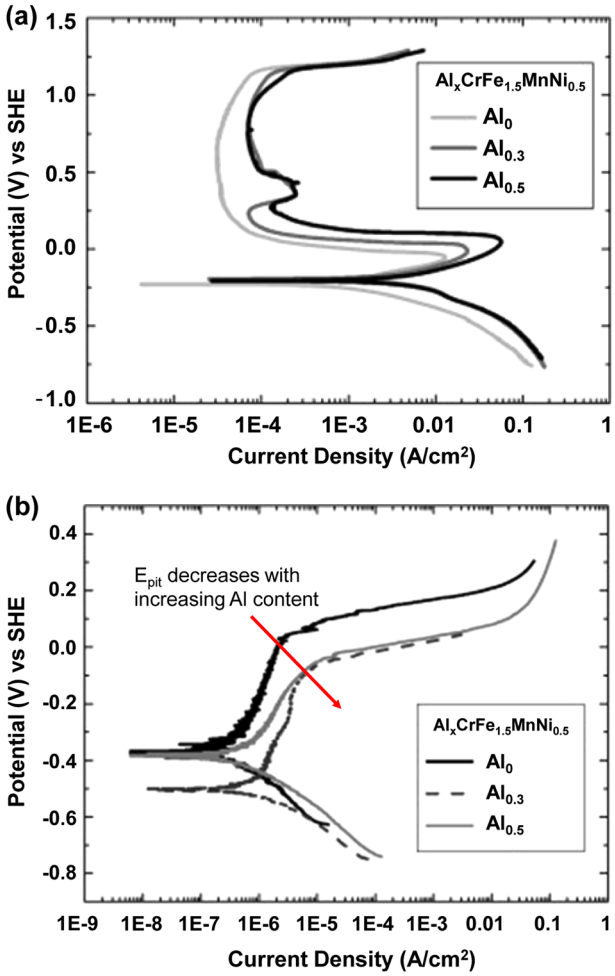

Fig. 2 **a** The effect of Al on the potentiodynamic polarisation response of the $Al_xCrFe_{1.5}MnNi_{0.5}$ system ($x = 0$, 0.3, 0.5) in 0.5 M H_2SO_4 (reprinted with permission from ref. 27). **b** A comparison of the potentiodynamic polarisation curves of the $Al_xCrFe_{1.5}MnNi_{0.5}$ system ($x = 0$, 0.3, 0.5) in 1 M NaCl (**a, b** reprinted from ref. 27 with permission from Elsevier)

study. Lee et al.[27] observed that the dimensions of the attacked/dissolved regions on the alloy surface, after polarisation (beyond breakdown) in 0.5 M H_2SO_4, was also increased with the Al content in spite of essentially the same E_{pit} values (Fig. 3).

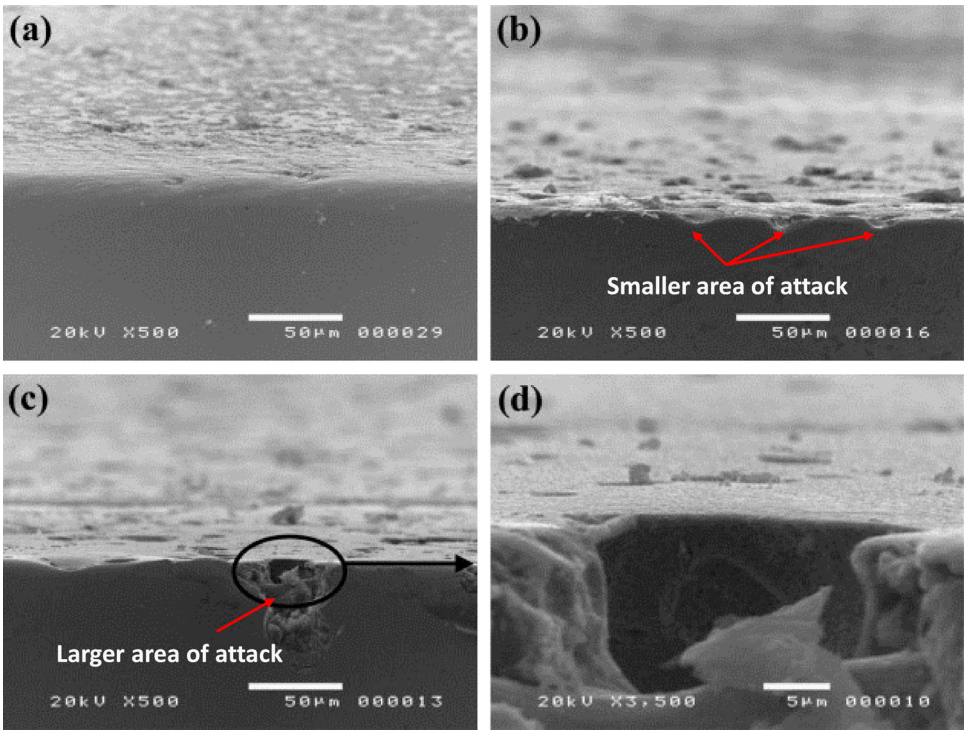

Fig. 3 The SEM micrographs for the $Al_xCrFe_{1.5}MnNi_{0.5}$ alloys with different molar concentrations of Al, after the anodic polarisation exceeded the breakdown potential (>1.25 V_{SHE}) in 0.5 M H_2SO_4 **a** $x = 0$, **b** $x = 0.3$ mol, **c** $x = 0.5$ mol, **d** a *higher magnification image* of the inset in micrograph **c** (**a–d** reprinted from ref. 27 with permission from Elsevier)

The E_{pit} values of the $Al_xCrFe_{1.5}MnNi_{0.5}$ alloys in 1 M NaCl solution were found to be decreased (to less noble values) compared to that of Al-free alloy $CrFe_{1.5}MnNi_{0.5}$ (Fig. 2b). A first-order assessment would suggest that an increase in the Al content may increase the pitting susceptibility of the CCA; however, it is noted that the Al-containing $Al_xCrFe_{1.5}MnNi_{0.5}$ alloy still displays considerable passivity in concentrated 1 M NaCl, and that E_{pit} is not the prime measure of pitting susceptibility. More interestingly, cyclic polarisation was able to reveal that the Al-free $CrFe_{1.5}MnNi_{0.5}$ alloy revealed negative hysteresis during cyclic potentiodynamic polarisation (CPP) in a 0.5 M H_2SO_4 + 0.25 M NaCl, indicating that a protective passive film forms upon the surface of this alloy, and repassivation is possible; however, the $Al_{0.3}CrFe_{1.5}MnNi_{0.5}$ alloy showed positive hysteresis during CPP in the same solution, revealing that repassivation may be hindered by dissolution altering surface chemistry. It does, however, merit comment that the alloys synthesised in the study of Lee et al.[27] were all found to have different microstructures. The Al-free alloy $CrFe_{1.5}MnNi_{0.5}$, with the lowest i_{corr} (6.86×10^{-4} A/cm^2) among the tested alloys, was found to have both an FCC solid solution phase with α-FeCr features. The $Al_{0.3}CrFe_{1.5}MnNi_{0.5}$ alloy was found to consist of both FCC and BCC phases, whereas the $Al_{0.5}CrFe_{1.5}MnNi_{0.5}$ alloy comprising a single BCC phase. The authors proposed that the FCC-type microstructure (as seen in the $CrFe_{1.5}MnNi_{0.5}$ alloy) was more corrosion-resistant than the BCC-type microstructure (in the $Al_xCrFe_{1.5}MnNi_{0.5}$ alloys), perhaps adopting the rationale that austenitic (FCC) stainless steel is more corrosion-resistant than ferritic (BCC) stainless steel.[27] However, such a hypothesis was not validated in that body of work. Also, the mechanism by which Al content influences the corrosion of the HEA was not clearly elaborated.

Kao et al.[28] investigated the passivation of the $Al_xCoCrFeNi$ alloys (with $x = 0$, 0.25, 0.5, 1) in 0.5 M H_2SO_4 solutions, with different chloride content ranging from 0.25 to 1 M. The Al content in the test alloys was 0, 3.05, 5.59 and 10.02 wt. %, respectively. Potentiodynamic polarisation tests revealed the presence of well-defined passive region between 0 and 1.2 V_{SHE} for all the tested alloys in 0.5 M H_2SO_4 solution. However, the steady-state passive current densities (i_{pass}) were found to steadily increase with increasing wt. % of Al in the alloy. The mass loss rates (from 8- to 15-day exposures) of the alloys with >5 wt. % Al in the H_2SO_4 solutions were also higher than those of the alloys with lower Al content. It was hypothesised that the increase in Al content increased the thickness of the passive film formed upon this HEA, thus correspondingly increasing the i_{pass} observed in the potentiodynamic polarisation tests. It was also observed that the E_{pit} of all the alloys decreased in the presence of Cl^- ions. The alloys were characterised by SEM/EDS both before and after immersion to observe the alloy microstructure and also to detect changes in chemical composition of the alloy after corrosion. An example of the characterisation for the $Al_{0.5}CoCrFeNi$ alloy is shown in Fig. 4.

It was observed that the alloys with 0 and 3.02 wt. % Al had a single FCC phase, whereas the alloy with 5.59 wt. % Al had a duplex FCC + BCC microstructure. The 10.02 wt. % Al-containing alloy had a complex BCC + B2 microstructure. It was identified that the Al and Ni content was lower following immersion in the test solution for the 5.59 wt. % and 10.02 wt. % Al-containing alloys. It was therefore proposed that a selective dissolution of the Al- and Ni-rich phase occurs for such alloys during exposure to acidic solutions.

The corrosion characteristics of the alloy $FeCoNiCrCu_{0.5}Al_x$ (x = 0.5, 1 and 1.5) in both 0.5 M NaCl and 0.5 M H_2SO_4 solution was investigated by Li et al.,[29] where 'x' denotes the molar ratio of Al in the alloys. It was observed that the phase structure of the $FeCoNiCrCoCu_{0.5}Al_x$ evolves from the FCC phase to the BCC phase, with the addition of Al. The as-cast $Al_{0.5}$ alloy was observed to consist of a single FCC phase, whereas the $Al_{1.0}$ alloy consisted of a BCC phase. The $Al_{1.5}$ alloy was observed to comprise both FCC and BCC phases. The $Al_{0.5}$ and $Al_{1.0}$ alloys were found have higher

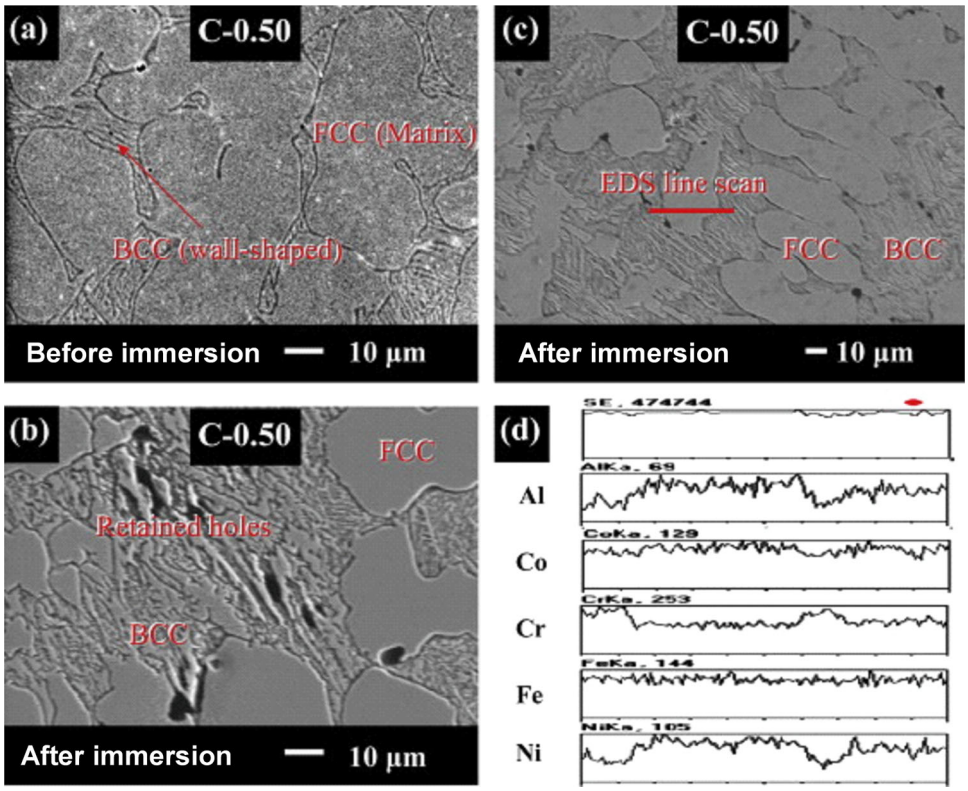

Fig. 4 **a** SEM image of $Al_{0.5}CoCrFeNi$ (C-0.50), **b**,**c** corrosion morphology of $Al_{0.5}CoCrFeNi$ alloy after 3-day immersion in 0.5 M H_2SO_4, **d** *EDXS line-scan* results of the location indicated in (**c**). Retained *holes* were from cast procedure (**a–d** reprinted from ref. 28 with permission from Elsevier)

corrosion current density (i_{corr}) values than the $Al_{1.5}$ alloy in the 0.5 M NaCl solution. However, the corrosion resistance increased in the order $Al_{1.0}$ >$Al_{0.5}$ >$Al_{1.5}$ in 0.5 M H_2SO_4 solution, with the $Al_{1.0}$ alloy having a lower i_{corr} than the $Al_{0.5}$ alloy. Li et al.[29] therefore proposed that the BCC phase was more corrosion-resistant than the FCC phase in the chloride and acidic solutions. The comparatively inferior corrosion resistance of the $Al_{1.5}$ alloy was attributed to microstructural heterogeneity owing to presence of the BCC + FCC duplex phase.

On the lines of work reported to date, it is unclear how detrimental, if at all, the addition of Al is to CCAs. The lines of work to date reveal that rather subtle changes in i_{corr} occur, and that Al does not alter the ability of CCAs to passivate. Nonetheless, Al has been shown to lead to microstructural changes, which in turn, were manifested to result in selective dissolution of Al and Al-rich phases. Given the ability of Al to reduce the density of CCAs rather dramatically, the effects of Al on the corrosion mechanism of the Al-containing CCAs are not yet well clarified.

The influence of titanium on the corrosion of CCAs. Pure titanium (Ti) is nominally a passive metal in most aqueous environments, as it spontaneously develops a protective TiO_2-based film upon its surface.[30] The addition of Ti to HEAs may be anticipated to improve resistance to corrosion, in cases when Ti is incorporated into the surface film.[31] Titanium is however 'metallurgically active' (in the melt) and tends to form several intermetallic compounds with the other elements in CCAs.[7, 12, 32–36] The presence of Ti results in the formation of the Fe_2Ti-type Laves phase in the $AlCoCrFeNiTi_{1.5}$[32] and CoCrCuFeNiTi systems.[33] There also exist reports of Ti promoting the formation of the $Ni_{2.67}Ti_{1.33}$-type R phase, the FeCr-type sigma phase and the Co_2Ti-type Laves phase in the $CoCrFeNiTi_{0.5}$ alloy.[7] The microstructure of many Ti-containing CCAs can therefore become more heterogeneous, due to the formation of such incorporating intermetallic compounds—with attendant ramifications for corrosion resistance.

The potentiodynamic polarisation curves of $CoCrFeNiAl_{0.9}$, CoCrFeNi and $Ti_{0.3}(CoCrFeNi)_{0.7}$ CCAs in 0.6 M NaCl are displayed in Fig. 5a.[18] Although these CCAs have a relatively similar composition, they exhibit significant differences in terms of their electrochemical response. The width of the passive window ($E_{pit} - E_{corr}$) is different for these CCAs and varies as follows: $Ti_{0.3}(CoCrFeNi)_{0.7}$ >$CoCrFeNiAl_{0.9}$ >CoCrFeNi (SPS^). It is interesting to note that a relatively wider passive window of $Ti_{0.3}(CoCrFeNi)_{0.7}$ exists, in spite of the heterogeneous microstructure and significant elemental segregation associated with this CCA. The microstructure of this alloy contains a Ti-rich phase (denoted as 'A' in the BSE image of $Ti_{0.3}(CoCrFeNi)_{0.7}$ (Fig. 5g)). This particular phase as a Ti concentration ~62.8 at.%. The wider passive window of the Ti-containing CCA is therefore ascribed to the presence of Ti, which may promote the growth of the protective TiO_2 film upon the metal surface. The post-immersion morphologies of these Ti-containing CCAs were not characterised/discussed, thereby making it difficult for one to comment further on the mechanistic influence of Ti on the corrosion of these CCAs.

For the $Al_2CrFeCoCuNiTi_x$ system,[37] the Ti-containing CCAs had lower i_{corr} values than the Ti-free CCA in 0.5 M HNO_3 (Fig. 6). The i_{corr} values were also found to decrease with increasing Ti content. Interestingly, the addition of small amounts of Ti ($x = 0.2$) or Si ($x = 0.2$) deteriorated the general corrosion resistance of both the $Al_{0.3}CrFe_{1.5}MnNi_{0.5}Ti_x$ and $Al_{0.3}CrFe_{1.5}MnNi_{0.5}Si_x$ systems[34] in 0.6 M NaCl. This detrimental effect was attributed to the formation of intermetallic compounds in the CCA, which could promote localised corrosion. Overall, however, it can be surmised from the literature to date that Ti mitigates the general corrosion of CCAs; however, the presence of so-called 'nobler' Ti-containing

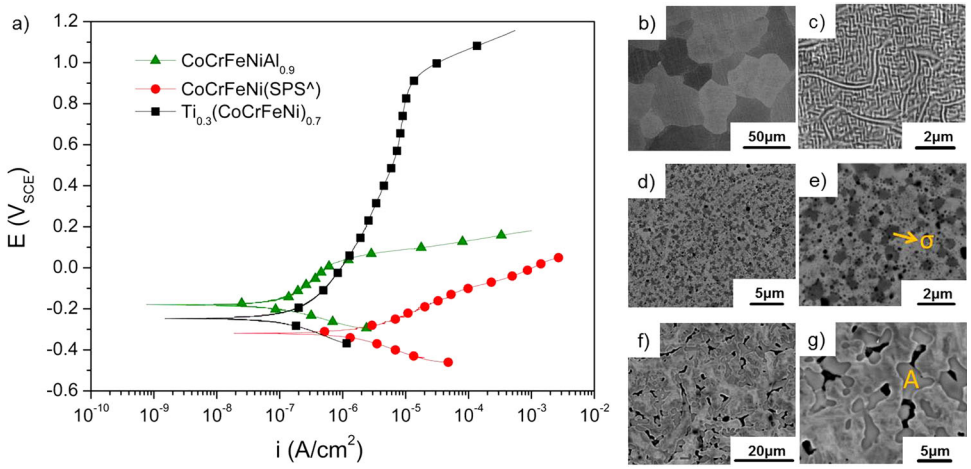

Fig. 5 **a** Polarisation curves for as-cast $CoCrFeNiAl_{0.9}$, CoCrFeNi and $Ti_{0.3}(CoCrFeNi)_{0.7}$ in 0.6 M NaCl at 25 °C, **b** BSE image of $CoCrFeNiAl_{0.9}$ at low magnification, **c** BSE image of $CoCrFeNiAl_{0.9}$ at *higher magnification*, **d** BSE image of CoCrFeNi at low magnification; this alloy was produced using spark plasma sintering, **e** BSE image of CoCrFeNi at higher magnification, **f** BSE image of $Ti_{0.3}(CoCrFeNi)_{0.7}$ at low magnification, **g** BSE image of $Ti_{0.3}(CoCrFeNi)_{0.7}$ at higher magnification (**a–g** reprinted from ref. 18 with permission from Taylor and Francis)

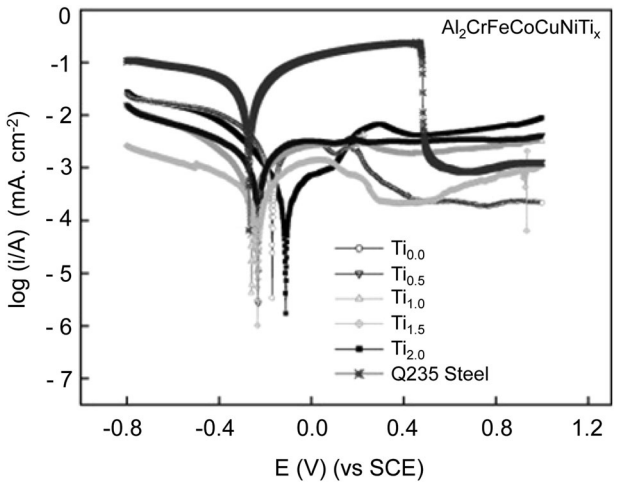

Fig. 6 The potentiodynamic polarisation curves for the $Al_2CrFeCoCuNiTi_x$system and Q235 steel (roughly equivalent to ASTM A36 mild steel) in 0.5 mol/l HNO_3 (reprinted from ref. 37 with permission from Elsevier)

phases dispersed within the CCA matrix may contribute to localised corrosion. An in-depth electrochemical characterisation of such phases using a local electrochemical technique such as the microcapillary electrochemical cell method[38–41] could provide more information on the role of such Ti-containing phases on the corrosion of CCAs.

The influence of chromium on the corrosion of CCAs. Chromium (Cr) is a primary alloying element in stainless steels (including Fe–Cr and Fe–Cr–Ni alloys) and CRAs (such as the Ni–Cr alloys). The addition of Cr makes these alloys 'stainless' as it forms a protective chromium oxide-based passive film upon the alloy surface.[42] The Cr loading in such alloys is critical to ensure that stainlessness is achieved. Shiobara et al.[43] observed that an applied potential >400 mV (vs SCE) is high enough to passivate Fe–Cr alloys, pure Fe and pure Cr in 1 M H_2SO_4. However, at lower applied potentials, pure Fe and low Cr-containing Fe alloys could not be passivated unless the Cr concentration was around 12–13 at.%. Newman et al.[44] performed anodic polarisation of Fe–Cr alloys (with varying Cr concentrations) in deaerated 1 M H_2SO_4 and observed that the decrease in the Fe-like behaviour of Fe–Cr alloys begins to occur when the Cr concentration is >9.5%. The complete disappearance of Fe-like behaviour occurs at around 17.5 at.% Cr. Asami et al.[45] used X-ray photoelectron spectroscopy (XPS) to characterise the composition and structure of the passive films formed upon Fe–Cr alloys, during polarisation (at 100 or 500 mV vs SCE) in deaerated 1 M H_2SO_4. They observed that for low Cr-containing Fe alloys, the passive film mainly comprised an iron oxide/hydroxide film. However, when the Cr at.% is >13% a hydrated Cr oxide/hydroxide forms upon the Fe–Cr alloy. The formation of this Cr oxide/hydroxide serves to passivate the ramified surface created by the selective dissolution of Fe during anodic polarisation[39] and is characterised by a well-defined passivation region in potentiodynamic polarisation curves.[39] The Cr_2O_3-based film also has a wide pH stability (between pH 2 and 12) and thus forms a protective insoluble barrier upon the metal.[46] Therefore, the Cr concentration must be >12 at.% in the case of Ni–Cr, Fe–Cr and Fe–Cr–Ni alloys for 'stainless' behaviour.[42]

The Cr concentration in Cr-containing CCAs is typically higher than 12%, and it is therefore plausible that Cr-containing CCAs have corrosion resistance (akin to Fe–Cr–Ni and Ni–Cr alloys)—should the hitherto unknown threshold for stimulation of a chromium oxide passive film in CCAs be fulfilled. In fact, the $Co_{1.5}CrFeNi_{1.5}Ti_{0.5}Mo_{0.1}$ alloy has a very high general corrosion and pitting resistance, with the E_{pit} values of these alloys being >0.5 V_{SHE}, in 1 M NaCl for temperatures ranging from 20 to 80 °C.[47] The intrinsic corrosion behaviour of such a CCA and how it derives from surface films or the intersolubility of Cr in the other alloying elements remains unknown. Al and Cu (among other elements such as Co, Fe and Ni) tend to lower the corrosion resistance of Cr-containing CCAs. The E_{pit} of the $Cu_{0.5}NiAlCoCrFeSi$ alloy containing Al, Cu and Cr in 1 M NaCl is well below <0 V_{SHE}.[17] Similarly, for $Al_xCrFe_{1.5}MnNi_{0.5}$, the E_{pit} values drop below 0 V_{SHE} when the Al molar ratio is >0.3.[27] The AlCoCrFeNi system was also observed to have relatively poor corrosion resistance in 3.5 wt. % NaCl. The alloy was found to have an interdendritic microstructure, with a Cr-depleted (and Al-rich) dendritic region and Cr-rich interdendritic region.[48] The Al-rich dendritic regions also had some Cr-rich precipitates dispersed within them, with the inferior relatively poor resistance of this alloy being attributed to a heterogeneous microstructure. It was proposed that the Al-rich regions become anodic and the Cr-containing regions become cathodic during exposure to an aqueous solution, resulting in the selective dissolution of the Al-rich phase in this alloy (Fig. 7). The presence

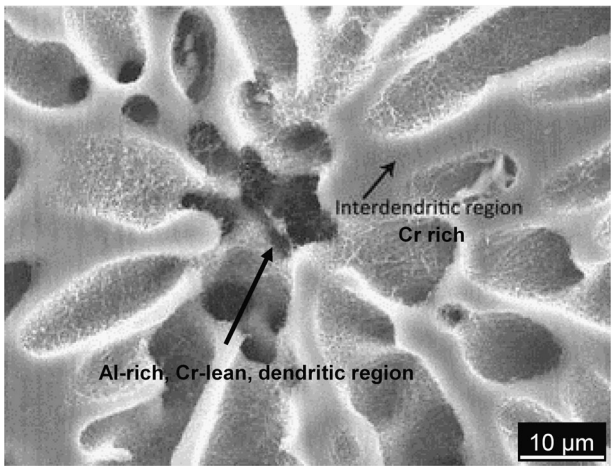

Fig. 7 The surface of an as-cast AlCoCrFeNi specimen after the potentiodynamic polarisation testing in 0.6 M NaCl. The image shows that the Cr-depleted dendrites experience selective dissolution, while the Cr-rich interdendritic regions remained largely unaffected (reprinted from ref. 48 with permission of Springer)

of Cr as a principal alloying element does not implicitly imply that Cr-containing CCAs are highly 'stainless', nor that a protective chromium oxide (Cr_2O_3) film is formed upon the alloy surface. The impact of other alloying elements on the corrosion characteristics and passivity of the alloy also needs to be considered. The native oxide or passive film formed upon the CCA could predominantly be that of the most reactive element (or in an aqueous context, the least noble element) in the CCA, with the other elements dispersed into the oxide in either their oxidised or unoxidised states. The surface films formed upon typical CCAs need to be extensively characterised to estimate their chemical compositions and to ratify their correlation with the alloy composition—a key area identified as a present knowledge gap.

The influence of molybdenum on the corrosion of CCAs. It is well-known that molybdenum (Mo) serves to improve the passivity and pitting resistance of austenitic stainless steels.[49] Pure Mo has been purported to form a protective MoO_2-based passive film or can generate MoO_4^{2-} species, which could reduce to the MoO_2 film at pit sites.[50, 51] Elemental Mo can also favour pit repassivation in stainless steels.[52] However in HEAs/CCAs, Mo tends to form a Mo and Cr-rich sigma (σ) phase,[53, 54] which could remove both Cr and Mo from the alloy matrix. This could be detrimental to the corrosion resistance of such Mo-containing CCAs if such a σ phase is present.

Chou et al.[54] evaluated the influence of Mo on the corrosion of $Co_{1.5}CrFeNi_{1.5}Ti_{0.5}Mo_x$ alloys in different solutions, namely deaerated 0.5M H_2SO_4, 1 M NaOH and 1 M NaCl by performing potentiodynamic polarisation tests. The wt. % of Mo in the synthesised CCAs was varied from 0 to 19.94%. The corrosion characteristics of the Mo-free and Mo-containing CCAs were fairly similar in the deaerated 0.5 M H_2SO_4 solution (Fig. 8a); however, in 1 M NaOH there was a slight increase in i_{corr} and a decrease in E_b (breakdown potential) values for the Mo-containing CCAs. For example, the i_{corr} of the $Co_{1.5}CrFeNi_{1.5}Ti_{0.5}Mo_{0.8}$ alloy (with 19.94 wt. % Mo) was found to be 0.25 μA/cm^2, which is slightly higher than that of $Co_{1.5}CrFeNi_{1.5}Ti_{0.5}Mo_0$ (0.09 μA/cm^2). The $Co_{1.5}CrFeNi_{1.5}Ti_{0.5}$ and $Co_{1.5}CrFeNi_{1.5}Ti_{0.5}Mo_{0.1}$ alloys comprised a single FCC phase, while the $Co_{1.5}CrFeNi_{1.5}Ti_{0.5}Mo_{0.5}$ and $Co_{1.5}CrFeNi_{1.5}Ti_{0.5}Mo_{0.8}$ were found to consist of the FCC as well as a Cr- and Mo-rich σ phase. The slightly lower corrosion resistance of these two alloys (in comparison with the Mo-free $Co_{1.5}CrFeNi_{1.5}Ti_{0.5}$ alloy) in 1 M NaOH solution was attributed to the presence of the σ phase, which could cause local Cr/Mo depletion in the alloy

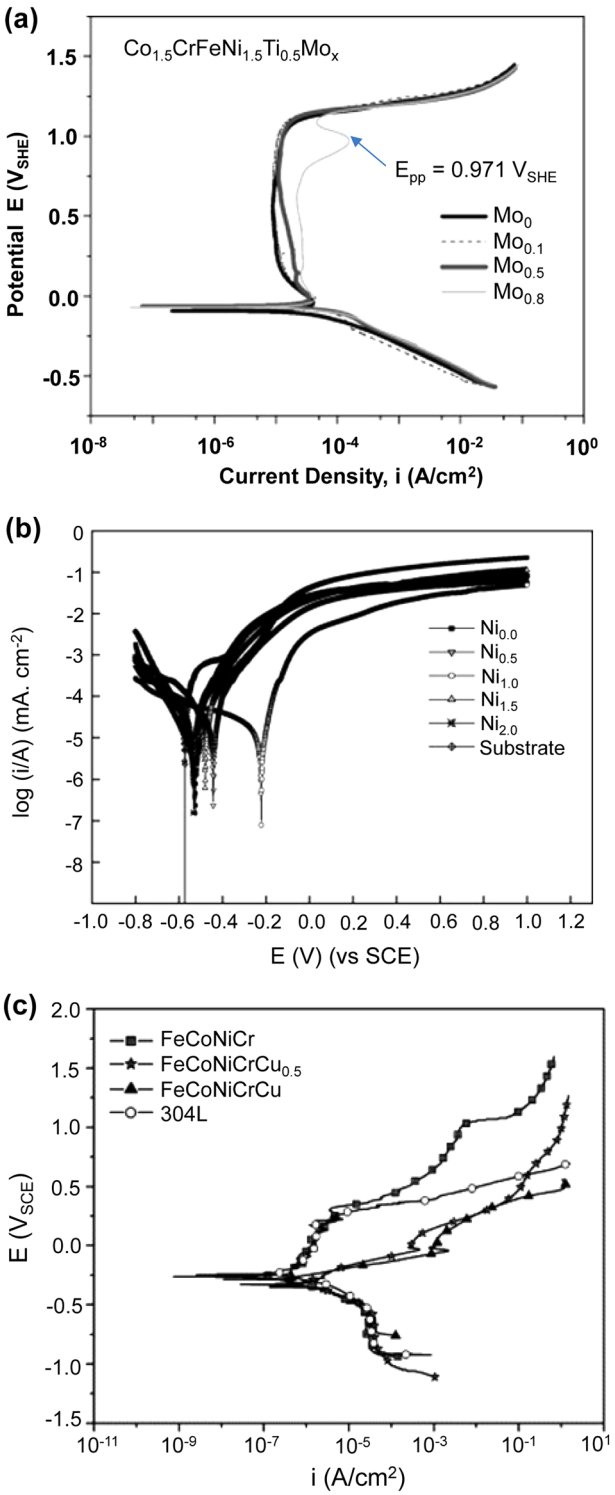

Fig. 8 **a** The potentiodynamic polarisation curves of the $Co_{1.5}CrFeNi_{1.5}Ti_{0.5}Mo_x$system with different Mo contents (where $x = 0$, 0.1, 0.5 and 0.8 mol) in deaerated 0.5 M H_2SO_4 (pH < 1; reprinted with permission from ref. 54). **b** The potentiodynamic polarisation curves for the $Al_2CrFeCoCuTiNi_x$ system in 3.5% NaCl (reprinted with permission from ref. 57). **c** Potentiodynamic polarisation curves of as-cast $FeCoNiCrCu_x$ alloys and 304 l in 3.5% NaCl at 25 °C (**a** reprinted from ref. 54 with permission from Elsevier; **b** reprinted from ref. 57 with permission from Elsevier; **c** reprinted from ref. 58 with permission from Elsevier)

matrix. The Mo-containing CCAs were found to be significantly better than the Mo-free CCA, in terms of the pitting resistance as judged by CPP in deaerated 1 M NaCl.[54] The E_b values of the Mo-containing CCAs were in the range 1.1–1.2 V_{SHE}, which is significantly more noble than the E_b of the Mo-free alloy (0.33 V_{SHE}). The Mo-containing CCAs also exhibited a significantly wider passive window (~ 1400 mV_{SHE}) than the Mo-free CCA (~ 550 mV_{SHE}). Mo-containing CCAs also revealed negative hysteresis during CPP in deaerated 1 M NaCl, while the Mo-free CCA showed a positive hysteresis. This clarifies that Mo addition improves the pitting resistance of the $Co_{1.5}CrFeNi_{1.5}Ti_{0.5}Mo_x$ CCA system and also improves the self-repairing capabilities of the passive film. It was proposed that the MoO_4^{2-} species serves to inhibit pitting of the Mo-containing CCAs and promotes formation of the Cr oxide-based inner barrier layer,[55] thus resulting in the improved corrosion resistance of such Mo-containing CCAs.

The influence of nickel on the corrosion of CCAs. Nickel (Ni) is an important element used in the manufacture of stainless steels and CRAs. In stainless steels, one principal reasons for Ni additions is to stabilise the austenite phase, accompanied with a high Cr content.[49] Ni can be alloyed with a high content of metals known to improve corrosion resistance, such as Mo, Cr and Cu, while retaining its ductile FCC structure.[56] Some examples of the Ni-based alloys include the Ni-Cu systems (Monel) which are known for their corrosion resistance in sea-water, brackish water and resistance to biofouling. The Ni–Mo systems (Hastelloy) are highly resistant to acids such as the sulphuric/hydrochloric acids and also the Ni–Cr alloys (Inconel) have excellent resistance to caustic solutions and stress corrosion cracking.[56]

The impact of Ni addition on the corrosion of the $Al_2CrFeCoCuTiNi_x$($x = 0$, 0.5, 1, 1.5 and 2) system was investigated in 3.5 wt. % NaCl and 1 M NaOH.[57] The alloy with the Ni molar ratio ($x = 1$) was found to have the lowest i_{corr} in both the neutral and the alkaline solutions (Fig. 8b). The i_{corr} values increased when $x > 1$, implying that there is critical Ni content beyond which Ni has a detrimental impact on the corrosion of the CCA. It is recognised that Ni may combine with Al to form the Al^{-}Ni-rich B2 phase, which may also deteriorate the corrosion resistance of Ni-containing $Al_2CrFeCoCuTiNi_x$ alloys.[28] However, the $Al_2CrFeCoCuTiNi_x$ alloys were found to be comprising an FCC and BCC phase[57]—with the authors of that study hypothesising that inferior corrosion resistance of the Ni-containing HEAs is related to the small atomic radius of Ni, compared to the other constitutional elements. This would result in a large lattice distortion in alloys with high Ni content and thereby could significantly influence the alloy microstructure, which will thus influence the corrosion resistance of such Ni-containing CCAs. Such hypotheses, however, have neither been experimentally tested nor validated.

The influence of copper on the corrosion of CCAs. Several researchers have explored the influence the effect of copper (Cu) on the corrosion and electrochemical response of CCAs.[58–60] Hsu et al.[58] investigated the corrosion behaviour of the $FeCoNiCrCu_x$ system (with x taken as 0, 0.5 and 1) in 0.6 M NaCl and observed that increasing Cu content resulted in a higher i_{corr}, lower E_{corr} and lower E_{pit} values for this system (Fig. 8c).

Inspection of the literature to date also reveals that Cu-containing CCAs showed higher cathodic kinetics relative to Cu-free CCAs of like compositions.[18] The average corrosion rates of Cu-containing CCAs were additionally determined after a 30-day immersion in 3.5 wt. % NaCl. The mass loss rate was ordered according to FeCoNiCrCu>$FeCoNiCrCu_{0.5}$>FeCoNiCr. The $FeCoNiCrCu_x$ alloys all had an FCC matrix; however, Cu segregation was found to form an interdendritic Cu-rich phase in the Cu-containing CCAs.[58, 61–63] The microstructures of the FeCoNiCrCu and $FeCoNiCrCu_{0.5}$ alloy were therefore found to consist of the interdendritic Cu-rich phase and the dendritic Cu-lean (and Cr-rich) phase. After the 30-day immersion test in 3.5% NaCl solution, a number of small pits were observed on the surface of the Cu-free FeCoNiCr alloy; however, in the Cu-containing alloys the interdendritic phase was preferentially dissolved. The authors attributed the preferential attack of the interdendritic phase to microgalvanic corrosion caused by the segregation of Cu, which was ascribed to the positive binary mixing enthalpy of Cu with the other constitutional elements (namely Fe, Co, Ni and Cr).

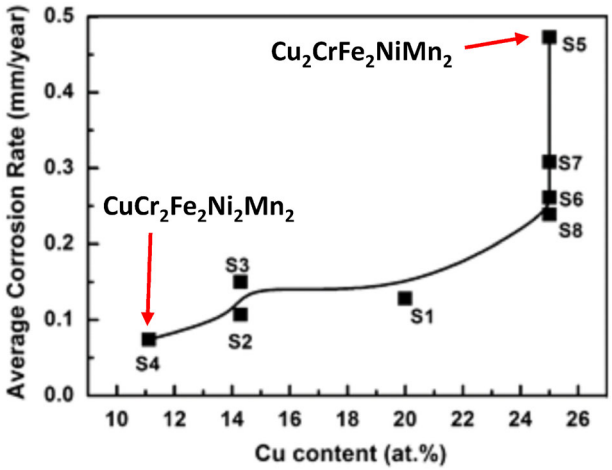

Fig. 9 Effect of Cu content on the corrosion rate (calculated from immersion tests) of different CuCrFeNiMn alloys (reprinted from ref. 59 with permission of John Wiley and Sons)

The effect of Cu on the corrosion of the CuCrFeNiMn system was also investigated by Ren et al.[59] using immersion tests and potentiodynamic polarisation tests in 1 M H_2SO_4. The $CuCr_2Fe_2Ni_2Mn_2$ alloy with a low Cu content and minimal elemental segregation had the highest corrosion resistance, whereas the $Cu_2CrFe_2Ni_2Mn_2$ alloy with the higher Cu content and more substantial elemental segregation had the poorest corrosion resistance. These alloys are labelled as S4 and S5, respectively, in Fig. 9. The surface morphologies of select alloys after a 100-h immersion in 1 M sulphuric acid (H_2SO_4) are shown in Fig. 10.

The authors claimed that the CuCrFeNiMn alloys experienced general corrosion and localised corrosion (including intergranular corrosion).[59] However, no elaboration on the nature of the phase (s) present at the grain boundaries—which preferentially corroded—was provided. It was proposed that the addition of Cu favours elemental segregation, thus increasing the corrosion rate of Cu-rich CCAs. In terms of the present review overall, it is salient to note that while microstructural heterogeneity per se is not in its own right problematic in the corrosion of CCAs (which was not necessarily expected); it is however apparent that large-scale segregation of elements can lead to localisation of corrosion. An independent study on the electrochemical properties of both the as-cast and aged $Cu_{0.5}CoCrFeNi$ alloy in 0.6 M NaCl revealed that, in addition to pitting, preferential dissolution of the Cu-rich phases also occurred (Fig. 11).[60] From the reports to date, it appears that Cu is detrimental to the corrosion resistance of CCAs as Cu promotes elemental segregation, forming a Cu-rich interdendritic phase and a Cu-lean (and Cr-rich in Cr-containing CCAs) dendritic phase.

The influence of boron on the corrosion of CCAs. Boron (B) is normally added to CCAs to improve their hardness and wear resistance, due to the ability of B to promote the formation of borides.[64] The addition of B to $Al_{0.5}CoCrCuFeNi$ was found to increase its hardness (Vickers hardness with a 5 kg load) to H_V 736 (from H_V 232 for the B-free alloy),[64] which is a considerable change. The wear resistance of this B-containing CCA was found

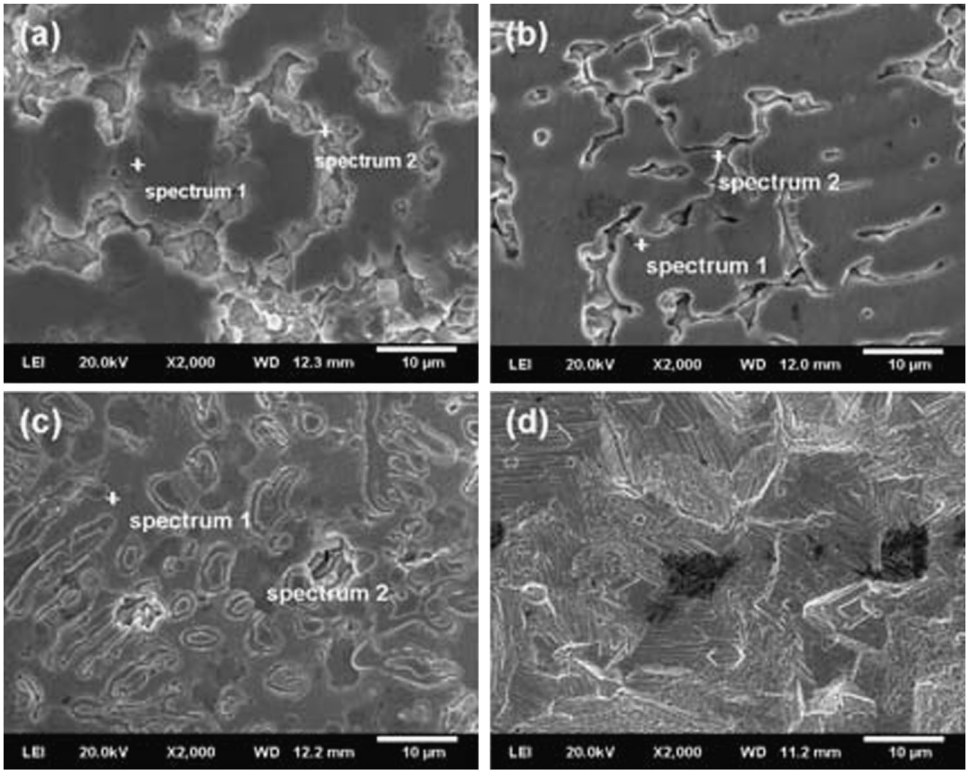

Fig. 10 Typical surface morphologies of the CuCrFeNiMn system after immersion tests in 1 M sulphuric acid for 100 h: **a** CuCrFeNiMn (S1), **b** $CuCr_2Fe_2Ni_2Mn_2$ (S4), **c** $Cu_2CrFe_2NiMn_2$ (S5), **d** 304 stainless steel (**a–d** reprinted from ref. 59 with permission of John Wiley and Sons)

to be much better than that of a SUJ2 wear-resistant steel.[64] The impact of B additions or borides on the corrosion of CCAs is not well-clarified or explored in any detail to date. The corrosion characteristics of the $Al_{0.5}CoCrCuFeNiB_x$ system in 1 N H_2SO_4 were however studied as a function of the B content, by Lee et al.[65] The B content in that study was varied from 0 at.% to 15.4 at.%. The CPP curves of the $Al_{0.5}CoCrCuFeNiB_x$ alloys revealed negative hysteresis, indicating that these alloys are not susceptible to localised corrosion for the test conditions explored, in spite of the acid concentration (Fig. 12a–d).

However, the i_{corr} values of the alloys were found to increase with the B content in the alloy. The repassivation potential (E_{rp}) of the alloys was also found to decrease with increasing B content (Fig. 12). This indicates that B does have some impact on the corrosion resistance of the $Al_{0.5}CoCrCuFeNiB_x$ CCA. Interestingly, however, the trend in corrosion characteristics was not similar for another B-containing system $FeCrNiCoB_x$.[66] The potentiodynamic polarisation tests in 0.6 M NaCl revealed the initial addition of B ($0.5 \leq x \leq 1.0$) lowered the corrosion rate of the alloy, despite the existence of a $(Cr, Fe)_2B$ compound in the alloy microstructure. Greater B additions ($x = 1.25$) did however increase the corrosion rate of the $FeCrNiCoB_x$ alloy. Explanations of such observed behaviours were not detailed; however, the authors suggested that $(Cr, Fe)_2B$ with an orthorhombic structure was more noble than the FCC matrix, and therefore beneficial for corrosion resistance. The apparently poor corrosion resistance of the $FeCrNiCoB_{1.25}$ alloy was attributed to the phase transformation of the boride from the aforementioned orthorhombic $(Cr, Fe)_2B$ phase to a tetragonal $(Fe, Cr)_2B$ phase—the authors do not however test or validate this hypothesis.

The influence of tin on the corrosion of CCAs. The addition of tin (Sn) has been found to increase the tensile strength of CCAs based on the CoCuFeNi and AlCoCrFeNi systems.[67, 68] The impact of Sn additions on the corrosion of the FeCoNiCu system was studied by Zheng et al.[69] The i_{corr} values of the Sn-containing FeCoNiCu alloys in 3.5 wt. % NaCl were found to be lower than those of 304 SS in the same solution, with the lowest i_{corr} observed for the FeCoNiCu alloy with a 0.03 molar ratio of Sn (Fig. 13a). The E_{pit} values of the Sn-containing alloys were however notably lower than the E_{pit} of 304 SS. Conversely, in 5% NaOH, the Sn-containing FeCoNiCu alloys revealed a higher i_{corr} and lower E_{pit} values than 304 SS in the same solution (Fig. 13b). In the case of testing in 5% NaOH, the FeCoNiCu alloy with a 0.04 molar ratio was found to have the lowest i_{corr}. The mechanistic effects of Sn on the corrosion characteristics of the CCAs were, however, not further clarified or discussed in that study, and nor was any detailed surface characterisation executed.

The influence of processing methods on the corrosion of CCAs

The influence of anodising on the corrosion of CCAs. The CCAs reported to date nominally comprise one or more of the so-called passive metals, which, in pure form, produce a protective film upon their surface. How the phenomenon is fundamentally altered in the presence of several other elements in equiatomic proportions, including non-passive metals, is unknown. In the case of metals with low passivation tendencies or limited passivity, anodising is often industrially applied. Employing this rational, the anodisation of CCAs was explored with the view of developing a superior protective film upon the alloy surface. A series of $Al_xCrFe_{1.5}MnNi_{0.5}$ alloys were anodisation treated in 15% sulphuric acid solution at constant potential of 700 mV_{SHE} for a period of 1800 s, with the aim of developing a protective layer upon the CCA surface.[70] The anodisation was confined within the passive region of the alloy that lies between 0.2 V_{SHE} and 1.1 V_{SHE} (Fig. 14a).[70] It was observed (using XPS) that a Cr_2O_3 oxide layer formed upon the surfaces of the anodisation treated $CrFe_{1.5}MnNi_{0.5}$ and

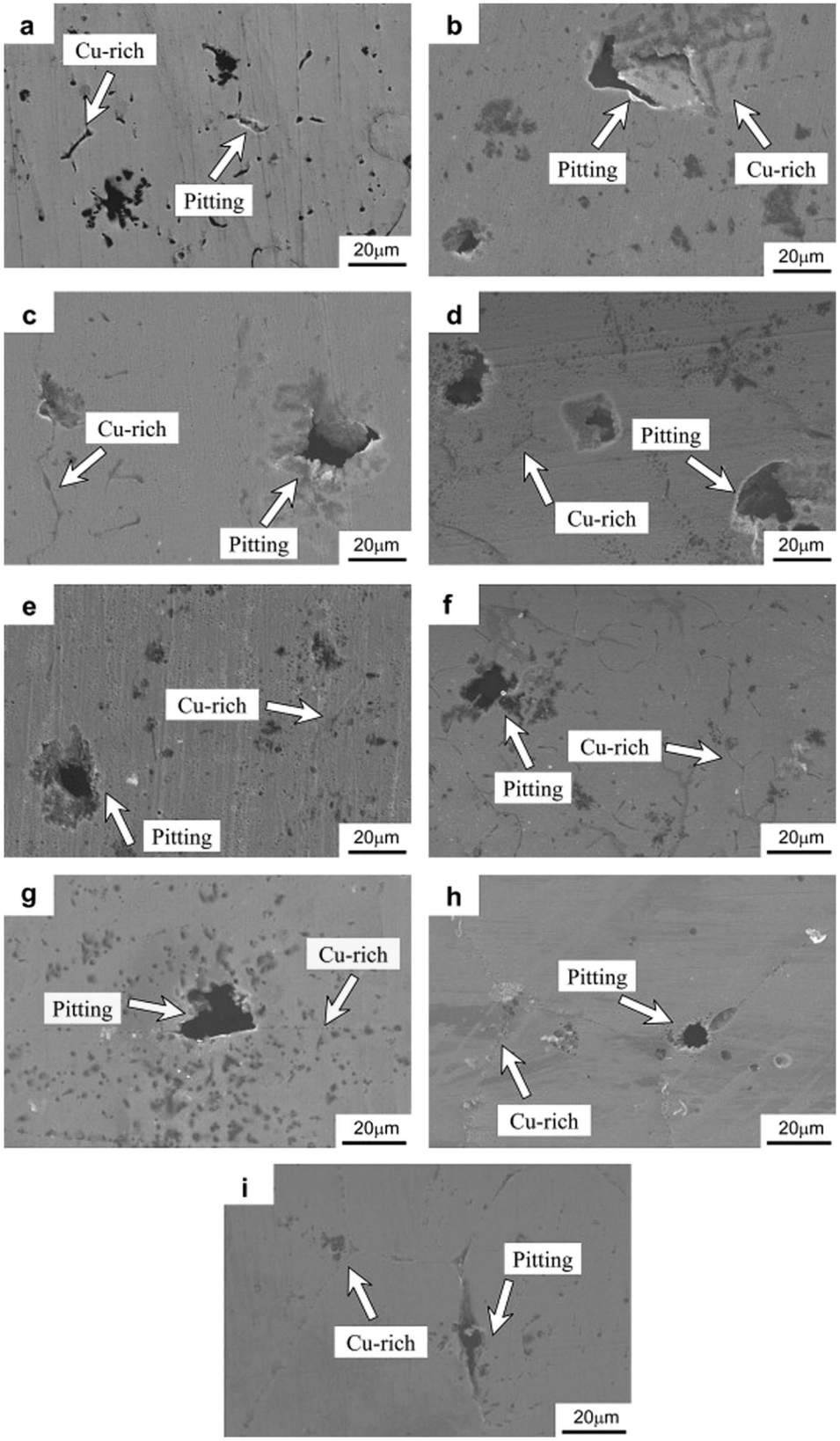

Fig. 11 Surface morphology of as-cast and aged $Cu_{0.5}CoCrFeNi$ alloys after potentiodynamic polarisation testing in 3.5% NaCl at 25 °C: **a** as-cast, **b** 350 °C, **c** 500 °C, **d** 650 °C, **e** 800 °C, **f** 950 °C, **g** 1100 °C, **h** 1250 °C, **i** 1350°C (**a–i** reprinted from ref. 60 with permission from Elsevier)

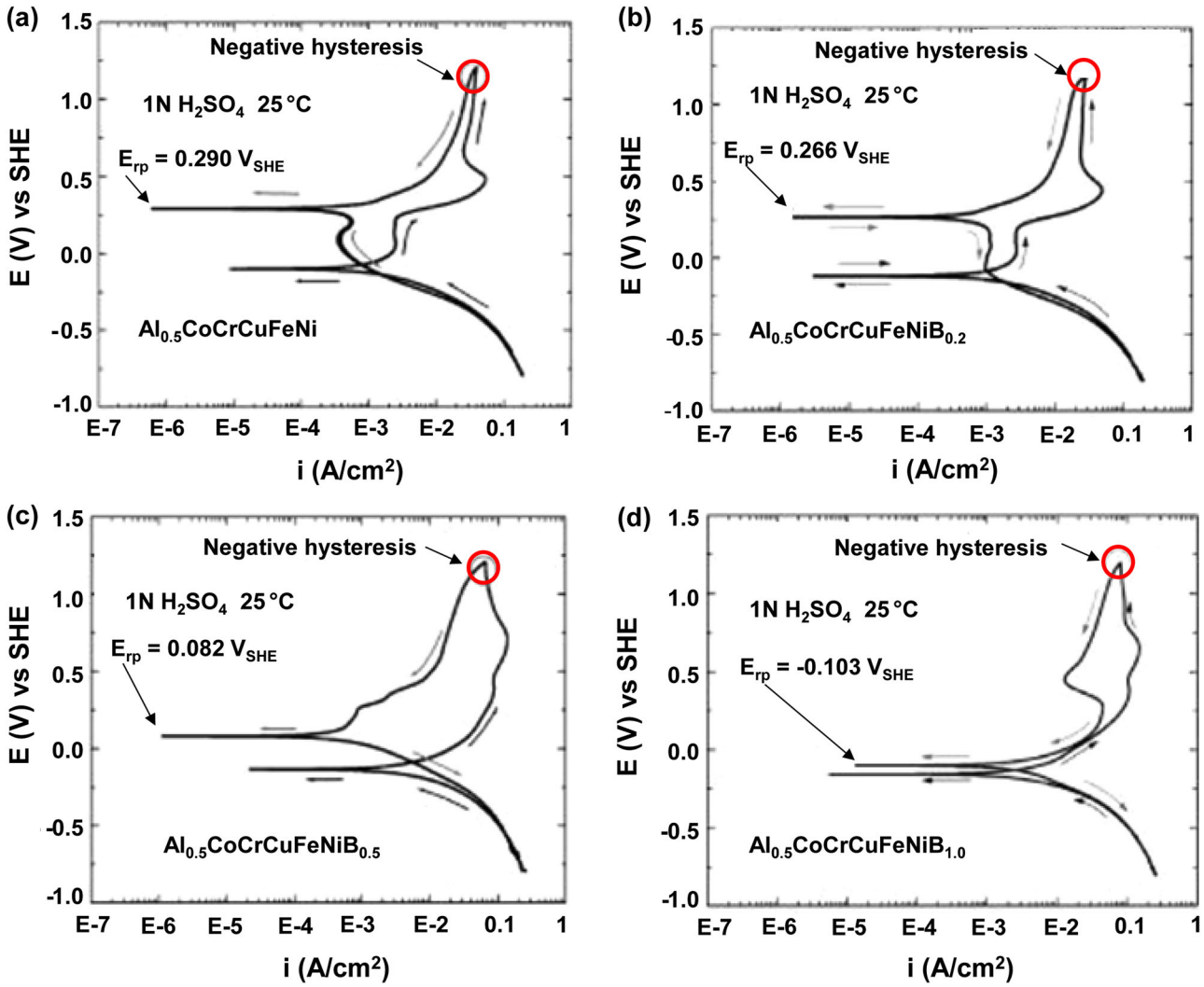

Fig. 12 Cyclic potentiodynamic polarisation curves of the $Al_{0.5}CoCrCuFeNiB_x$ system with different boron molar ratios: **a** $x = 0$, **b** $x = 0.2$, **c** $x = 0.6$ and **d** $x = 1.0$ mol in deaerated 1 N H_2SO_4 (**a–d** reproduced by permission of The Electrochemical Society from ref. 65)

$Al_{0.3}CrFe_{1.5}MnNi_{0.5}$ alloys. This layer formed by anodising was found to increase the corrosion resistance of these alloys in 0.1 M HCl, compared to the untreated (unanodised) alloys. EIS revealed that anodising increased the corrosion resistance of the $CrFe_{1.5}MnNi_{0.5}$ and $Al_{0.3}CrFe_{1.5}MnNi_{0.5}$ alloys by two orders of magnitude, compared to the untreated alloys in the Cl^--containing environment (akin to the effect of anodisation as reported on other alloys, leading to an insulating, thick, surface film). Anodising treatments with an aim to either enrich a passive metal on the CCA surface or develop a uniform passive film upon the CCA may be a useful approach to increase the corrosion resistance of CCAs—however, such studies remain scarce to date—as does the need for surface treatments on many CCAs that nominally also appear to be inherently corrosion-resistant.

The influence of aging on the corrosion of CCAs. Aging treatments are widely used for structural materials such as ferrous alloys, Al and Mg alloys, in order to tailor their microstructure to achieve the desired mechanical (and sometimes corrosion) properties.[71, 72] Several researchers have explored the effect of aging on the corrosion behaviour of CCAs.[60, 73] For the $Cu_{0.5}CoCrFeNi$ alloy,[60] it has been shown that aging at higher temperatures (1250 and 1350 °C) for 24 h improved the corrosion resistance of the alloy in 0.6 M NaCl, compared to aging at lower temperatures (350–1100 °C). It was proposed that the aging at higher temperatures, results in the dissolution of the Cu-rich FCC phase into the FCC matrix. This therefore minimises the ultimate Cu segregation in the alloy microstructure and improves corrosion resistance. For the Al-containing $Al_{0.5}CoCrFeNi$ alloy,[73] it was observed that the alloy aged at 650 °C exhibited the lowest corrosion rate when assessed by potentiodynamic polarisation, presenting the most noble E_{corr}, lowest i_{corr} and the highest E_{pit}, from tests in 3.5 wt. % NaCl solution (Fig. 14b). The aging treatment in this case restricted the distribution of the Al-Ni-rich phase and decreased the heterogeneity of the microstructure with increasing aging temperature. The surface morphologies of the as-cast and aged $Al_{0.5}CoCrFeNi$ alloy specimens following immersion in 3.5% NaCl (Fig. 15) validated that the Al–Ni rich phases were preferentially attacked by Cl^- containing electrolytes, while the FCC matrix remained essentially unaffected. It also merits comment that the $Al_{0.5}CoCrFeNi$ alloy aged 650 °C actually presented one of the highest hardness values and the greatest corrosion resistance among as-cast and aged alloys (noting that in a broader sense, mechanical and corrosion assessments are best coupled). Like any other metal alloy system, it can be concluded that aging will tailor the microstructure of CCAs, allowing phase evolution and solid-state

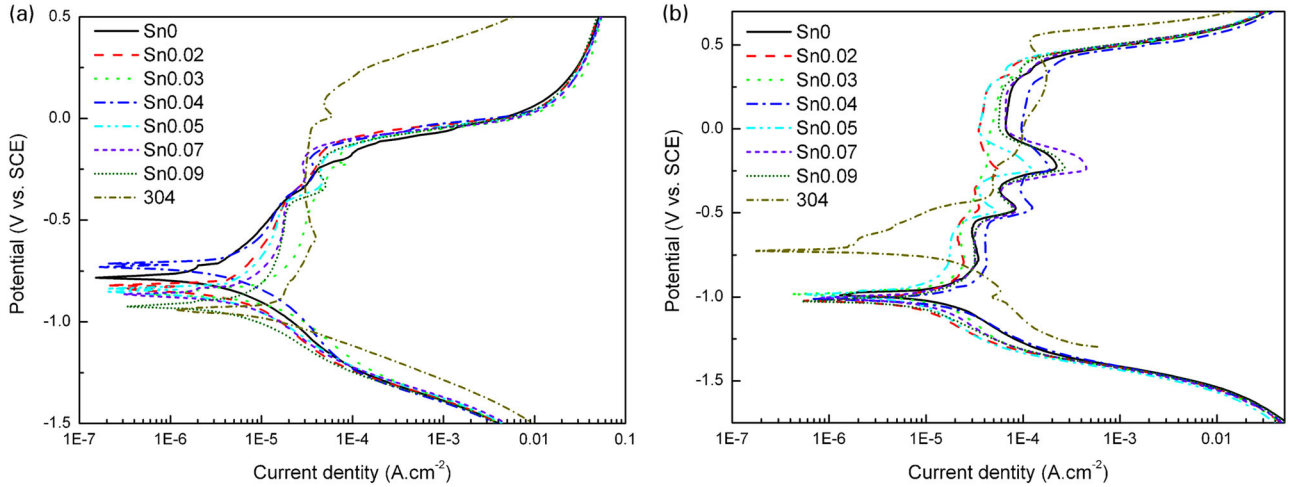

Fig. 13 Potentiodynamic polarisation curves of the $FeCoNiCuSn_x$ system and 304 SS in **a** 3.5 % NaCl; **b** 5 % NaOH (**a–b** reprinted from ref. 69 by permission of Taylor and Francis Ltd, copyright The Institute of Materials, Minerals and Mining)

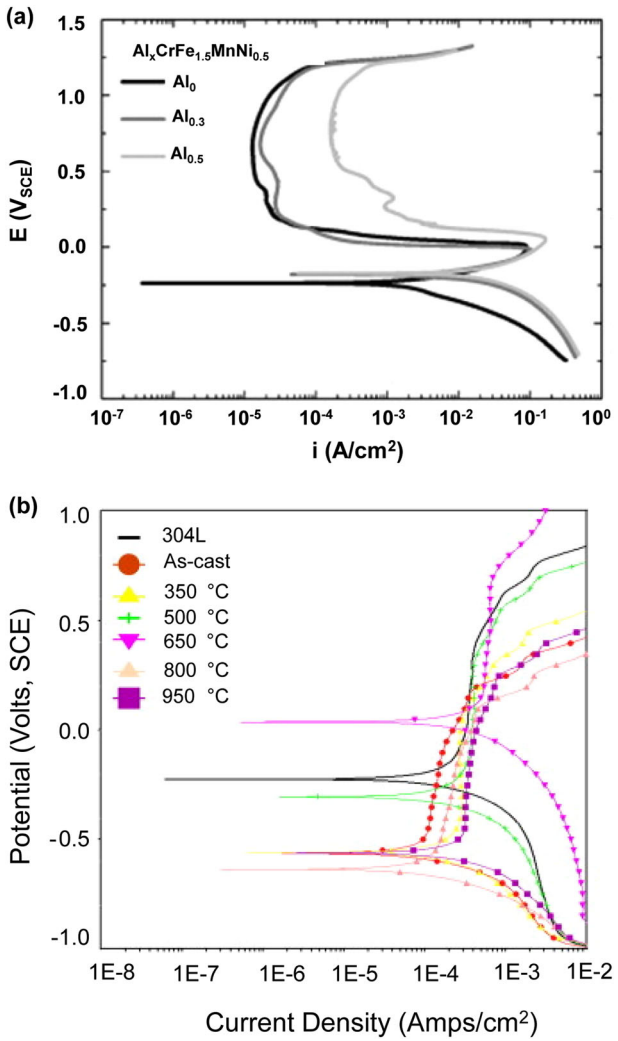

Fig. 14 **a** Effect of aluminium content in the $Al_xCrFe_{1.5}MnNi_{0.5}$ ($x = 0$, 0.3 and 0.5) system as determined by potentiodynamic polarisation curves in 15% H_2SO_4 solution. **b** The potentiodynamic polarisation curves of as-cast and aged $Al_{0.5}CoCrFeNi$ alloy specimens in 3.5 % NaCl solution at 25 °C (**a** reprinted from ref. 70 with permission from Elsevier; **b** reprinted from ref. 73 with permission from Elsevier)

dissolution. One complication to date, however, is that phase diagrams for CCAs do not generally exist. Phase diagrams would be beneficial in guiding aging treatments (and selection of aging temperatures). To date, it has been demonstrated that phase diagrams for CCAs may be produced by first principles modelling coupled with CALPHAD,[4, 74–76] and this is likely to be a fruitful area of future work.

GENERAL DISCUSSION

The nature of the testing reported in the literature to date makes it difficult to accurately compare the corrosion performance of the various CCAs reviewed. Studies to date have each had a unique focus, and employ a specific set of analyses. In regard to the latter point, the electrolytes/environments used for investigating the corrosion characteristics of CCAs vary remarkably (in ionic species, ionic concentration and pH), making it difficult to compare their relative corrosion performance. The conclusions, findings and even points surmised in the majority of research to date are general in nature, with only a minor focus given to the mechanistic aspects regarding corrosion of CCAs. The complex compositions (and variations of them) of the CCAs make it difficult to isolate the chemical effects of each individual element. This is evident from the sections above, where discussion regarding the effect of one element is not possible in isolation of the other elements in the CCA. Ideally to investigate the effect of a single alloying element on the corrosion of a CCA, its molar ratio needs to be carefully varied whilst the molar ratios of the other elements are kept fixed. This approach however would be rather tedious, and also needs to factor in second order effects such as phase changes. However, undoubtedly, the present literature review has been able to identify some of the most, and least, corrosion-resistant CCAs and to relate their corrosion characteristics to their elemental composition and microstructure.

The corrosion characteristics of a variety of CCAs reviewed have been summarised and tabulated in Table 1. This tabulation is a consolidated summation for the reader, indicating the variety of CCAs produced and tested to date, in addition to the type of electrolyte, and type of corrosion assessment employed. While the CCAs tested vary in composition, electrolyte, and test method, many studies have included benchmarking against known alloys (nominally stainless steels or ferrous alloys). To this end, the accompanying comments reveal rather unilaterally that CCAs, in spite of vast variations in chemistry and phase fractions, are nominally corrosion-resistant. This implies that they have the

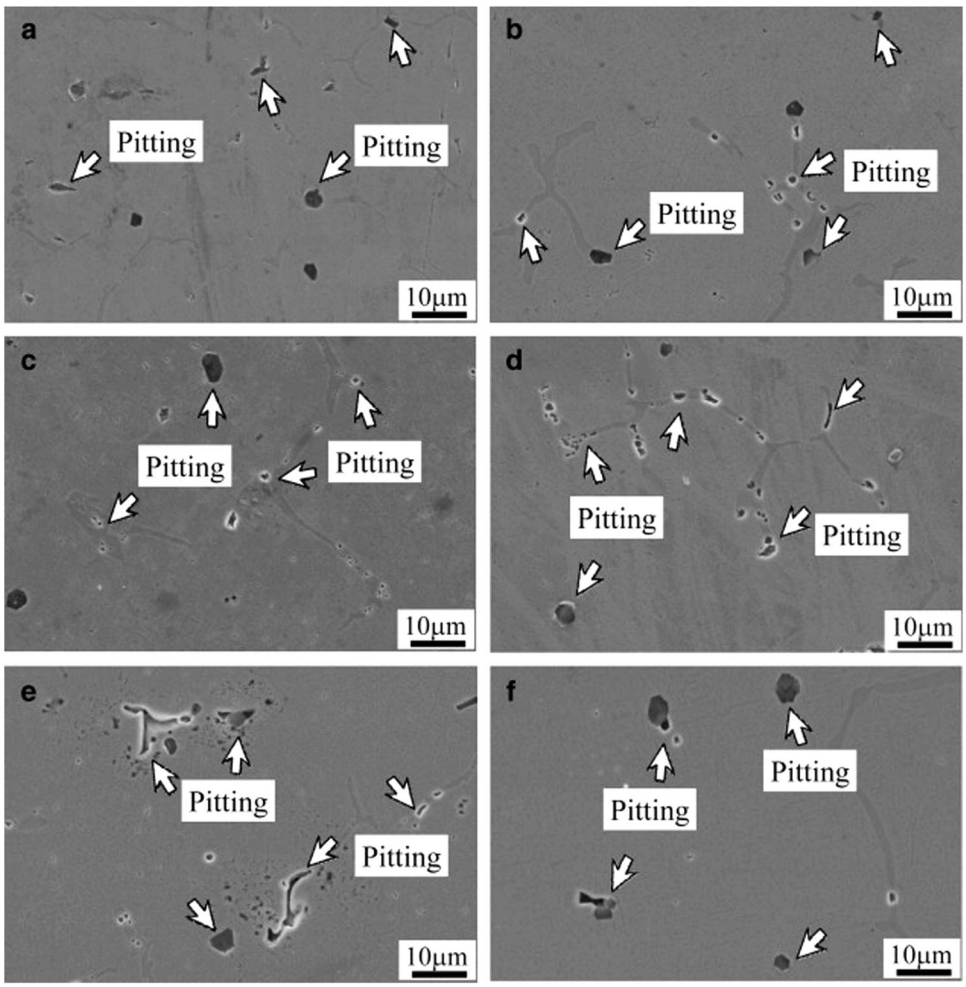

Fig. 15 The surface morphologies of as-cast and aged $Al_{0.5}CoCrFeNi$ alloy specimens following immersion in 3.5% NaCl solution at 25 °C: **a** as-cast, **b** 350 °C, **c** 500 °C, **d** 650 °C, **e** 800 °C and **f** 950 °C (**a**–**f** reprinted from ref. 73, with permission from Elsevier)

typical characteristics of so-called CRAs such as stainless steels, capable of passivation and sustained passivation over a range of potentials.

The E_{corr} and E_{pit} values of several CCAs in 0.6 M NaCl are also presented in Fig. 16. This essentially represents a galvanic series for the CCAs. The E_{corr} ranges of an austenitic stainless steel, ferritic stainless steel, mild steel and Al alloys are also indicated to enable a general comparison with the E_{corr} values of the CCAs in the same electrolyte. The E_{corr} values of many CCAs are in the range of those of austenitic and ferritic stainless steel. Also, the E_{pit} values of many of the CCAs are nobler than that of 304 SS.

$Ti_{0.3}(CoCrFeNi)_{0.7}$ was identified as one of the most corrosion-resistant CCAs, with a very low i_{corr} ($<10^{-8}$ A/cm^2). The Mo-containing CCAs namely $Co_{1.5}CrFeNi_{1.5}Ti_{0.5}Mo_x$ ($x = 0.1$ 0.5 and 0.8) also demonstrated excellent corrosion resistance. These alloys had noble E_{pit} values (>900 mV vs SCE), indicating that they have a very low susceptibility towards pit initiation. The $FeCoNiCuSn_x$ alloys were found to be one of the least corrosion-resistant systems, with i_{corr} values $>10^{-6}$ A/cm^2 and E_{pit} values <−400 mV vs SCE.

The literature surveyed in the present review tended to support the fact that elements such as Mo, Cr and Ti serve to lower the corrosion rate of CCAs. The role of Mo and Cr in protecting CCAs was posited to be similar to their protecting role in stainless steels; however, detailed analysis of such hypotheses remains lacking. It is still not categorically clarified whether a Mo, Ti or Cr-based oxide indeed forms upon these CCAs, as opposed to oxides of the other more reactive elements in these CCAs. The addition of elements such as Al, Cu and B was detrimental to the corrosion resistance of CCAs; however, the level of corrosion resistance alteration arising from Al additions was considered minor and not conclusive. Cu favours the formation of Cu-rich interdendrites in the CCA microstructure, which can differ in electrochemistry with Cu-lean (Cr-rich) dendrites, and is posited to influence the corrosion rate of Cu-containing CCAs. The segregation of Cu is due to the weak bonding of Cu with other elements indicated by the close to zero or positive binary mixing enthalpy.[58] The addition of B was revealed to cause the formation of borides in the microstructure, which were determined to undermine the corrosion resistance of B-containing CCAs. As highlighted herein, the effect of Al in Cr-containing CCAs is yet to be well clarified. For example, Cr has a low solubility in Al (maximum solubility is around 0.77 wt. %);[77] therefore, it is possible that several secondary phases or intermetallic compounds form in CCAs containing both Al and Cr, which could undermine the corrosion resistance of such CCAs. This aspect however needs to be clarified and balanced with any role Al may have in incorporation into surface films. Ti forms several intermetallic compounds that increases the heterogeneity of the CCA microstructure; however, their relative electrochemical difference to the matrix was postulated as being minor, and Ti additions tend to be overall beneficial to CCAs. Sn does not have a significant impact on the corrosion of CCAs for the compositions

Table 1. Tabulation of reported corrosion characteristics of some CCAs

System	Molar ratio (X)	Test					Electrochemical parameters			Localised corrosion	Comments	Reference
		OCP	Potentiodynamic polarisation	EIS	Mass loss	Electrolyte	E_{corr} (mV_{SCE})	i_{corr} (A/cm^2)	E_{pit} (mV_{SCE})			
$Al_xCrFe_{1.5}MnNi_{0.5}$	0 0.3 0.5	✗	✓	✓	✗	0.5 M H_2SO_4 1 M NaCl	−473 −438 −450	6.86×10^{-4} 2.39×10^{-3} 5.08×10^{-3}	✗ ✗ ✗	✗ ✓ ✓	High free corrosion rate reported, however an active-passive transition occurs. This leads to a wide passive region in acidic solution; Al reported to impair corrosion resistance in both electrolytes tested	27
$Al_xCoCrFeNi$	0 0.25 0.5 1	✓	✓	✓	✓	0.5 M H_2SO_4	−325 −339 −328 −338	15.8×10^{-6} 16.7×10^{-6} 13.4×10^{-6} 13.1×10^{-6}	✗ ✗ ✗ ✗	✓	Wide passive region. Better general corrosion resistance than 304 SS	28
$FeCoNiCrCu_{0.5}Al_x$	0.5 1 1.5	✗	✓	✗	✗	0.5 M NaCl 0.5 M H_2SO_4	−286 −288 −443	1.31×10^{-6} 8.21×10^{-7} 1.87×10^{-5}	✗ ✗ ✗	Not reported	As-cast $FeCoNiCrCu_{0.5}Al$ alloy exhibits better corrosion resistance than 321 SS in acidic solution based on potentiodynamic polarisation test	29
$Al_{0.3}CrFe_{1.5}MnNi_{0.5}Ti_x$	0 0.2	✗	✓	✗	✗	0.6 M NaCl	−230 −310	2.41×10^{-8} 7.34×10^{-7}	✗ ✗	Not reported	Small amount of Ti ($x=0.2$) addition deteriorates the corrosion resistance	34
$Al_{0.3}CrFe_{1.5}MnNi_{0.5}Si_x$	0 0.2	✗	v	✗	✗	0.6 M NaCl	−230 −300	2.41×10^{-8} 4.71×10^{-8}	✗ ✗	Not reported	Small amount of Si ($x=0.2$) slightly increased the corrosion rate	34
$Al_2CrFeCoCuNiTi_x$	0 0.5 1 1.5 2	✗	✓	✗	✗	0.5 M HNO_3	−180 −300 −330 −300 −150	3.8×10^{-5} 2.2×10^{-5} 7.3×10^{-6} 4.4×10^{-6} 2.7×10^{-6}	✗ ✗ ✗ ✗ ✗	Not reported	Better general corrosion resistance than Q235 steel (roughly equivalent to ASTM A36 mild steel)	37
As-cast AlCoCrFeNi		✗	✓	✗	✗	0.6 M NaCl	−294	9.30×10^{-8}	✗	✓	The Al-rich, Cr-lean dendrites suffer from selective dissolution. The alloy has better corrosion resistance than AISI 1045 steel	48
$Co_{1.5}CrFeNi_{1.5}Ti_{0.5}Mo_x$	0 0.1 0.5 0.8	✗	✓	✗	✗	0.5 M H_2SO_4, 1 M NaCl 1 M NaOH	−687 −625 −737 −795	5.7×10^{-7} 1.3×10^{-7} 2.0×10^{-7} 4.1×10^{-7}	94 970 920 938	✓	Mo-containing alloys are not susceptible to pitting corrosion in 1 M NaCl	54
$Al_2CrFeCoCuTiNi_x$	0 0.5 1 1.5 2	✗	✓	✗	✗	0.6 M NaCl 1 M NaOH	−510 −430 −220 −480 −500	6.8×10^{-5} 3.2×10^{-5} 1.3×10^{-5} 6.4×10^{-5} 6.7×10^{-5}	✗ ✗ ✗ ✗ ✗	Not reported	The general corrosion resistance increases up to $x=1$, and then decreases with further addition of Ni	57
$FeCoNiCrCu_x$	0 0.5 1	✗	✓	✗	✓	0.6 M NaCl	−260 −290 −330	3.15×10^{-8} 7.23×10^{-7} 1.32×10^{-6}	310 90 80	✓	Preferential dissolution of the Cu-rich FCC phase. FeCoNiCr alloy exhibits better general corrosion resistance than 304 L SS	58

Table 1 continued

System	Molar ratio (X)	Test					Electrochemical parameters			Localised corrosion	Comments	Reference
		OCP	Potentiodynamic polarisation	EIS	Mass loss	Electrolyte	E_{corr} (mV_{SCE})	i_{corr} (A/cm^2)	E_{pit} (mV_{SCE})			
$CuCr_2Fe_2Ni_2Mn_2$		✗	✓	✗	✓	1 M H_2SO_4	−974	2.09×10^{-6}	✗	✓	Higher Cu content and elemental segregation leads to higher corrosion rate	59
$Cu_2CrFe_2NiMn_2$		✗	✓	✗	✓	1 M H_2SO_4	−1144	4.02×10^{-5}	✗	✓		
$Cu_{0.5}CoCrFeNi$		✗	✓	✗	✗	0.6 M NaCl	−280	2.03×10^{-9}	70	✓	Lower corrosion resistance than 304l SS for both the as-cast and aged alloys	60
$Al_{0.5}CoCrCuFeNiB_x$	0 0.2 0.6 1	✗	✓	✓	✗	1 N H_2SO_4	−359 −365 −392 −403	7.87×10^{-4} 1.03×10^{-3} 2.63×10^{-3} 2.85×10^{-3}	✗ ✗ ✗ ✗	✓	Superior general corrosion resistance than 304 SS	65
$FeCrNiCoB_x$		✗	✓	✗	✗	0.6 M NaCl	✗	✗	✗	Not reported	Better general corrosion resistance than 304l SS	66
$FeCoNiCuSn_x$	0 0.02 0.03 0.04 0.05 0.07 0.09	✗	✓	✗	✓	0.6 M NaCl, 5% NaOH	−1030 −1089 −1097 −966 −1095 −1103 −1173	9.49×10^{-5} 2.13×10^{-6} 3.23×10^{-6} 9.69×10^{-5} 1.35×10^{-6} 1.86×10^{-6} 2.03×10^{-6}	−490 −397 −393 −421 −425 −414 −433	Not reported	Better corrosion resistance than 304 SS in NaCl solution. Poorer corrosion resistance than 304 SS in NaOH solution	69
$Al_xCrFe_{1.5}MnNi_{0.5}$		✗	✓	✓	✗	15% H_2SO_4 1 M HCl	✗	✗	✗	✓	Anodisation in 15 % H_2SO_4 significantly enhances the corrosion resistance	70
$Al_{0.5}CoCrFeNi$		✗	✓	✗	✗	0.6 M NaCl	−570	1.7×10^{-7}	130	✓	Cl^- ions preferentially attack the Al–Ni-rich phase	73
AlCrFeNiCoCu		✗	✓	✗	✗	1 M NaCl	−12	3.23×10^{-9}	✗	Not reported	Better general corrosion resistance than 304 SS	78
CoCrCuFeNiNb		✗	✓	✓	✗	1 M/6 M HCl	−397	8.93×10^{-5}	✗	Not reported	Better general corrosion resistance than 304 SS in HCl	79

For those CCAs tested in multiple electrolytes, the electrochemical parameters of one select electrolyte (not underlined) are presented

surveyed, whereas Ni is beneficial at molar ratios <1 but detrimental at molar ratios >1.

The corrosion resistance of CCAs was shown to be influenced (beneficially) by either anodising or appropriate aging treatments, both of which have a different desired outcome. Anodising serves to create a superior, thicker, surface film, formed under controlled conditions. It is noted that anodising is not common for CRAs, and as such, its application to a CCA is rather unique (anodising is nominally applied to Al alloys, but not to steels). The application of anodising to a number of CCA compositions would illuminate the relevance if such a surface treatment and if such a treatment relies on specific elements to respond to surface film development via anodising.

The application of aging (heat) treatments was shown to be able to alter the microstructure of CCAs, with attendant phase changes occurring in the solid state. Indeed, such aging treatments are metallurgically common for systems with known phase behaviour, which includes the majority of structural alloys used industrially. The testing of CCAs in the as-cast or as-solidified condition is common in studies of CCAs, but not considered best practice by conventional metallurgical wisdom. As such, the test matrix required for a better understanding of the corrosion of CCAs undoubtedly needs significantly more studies on the role of aging treatments—in collaboration with physical metallurgists to understand the phase evolution in CCAs.

FUTURE WORK

The corrosion characteristics of the CCAs have to date been screened using so-called global methods such as immersion tests, potentiodynamic polarisation and EIS testing. Such tests have been typically conducted in electrolytes that include as H_2SO_4, NaCl and NaOH. While a general appreciation of the relative corrosion performance of CCAs can be gauged from the testing reported in the literature and presented herein, it is evident that significant future work is required to both (i) fully understand the corrosion of CCAs and (ii) harness that understanding into the development of CCAs with high corrosion resistance. Some aspects of necessary future work include the following.

- At the most basic of levels, studies that assess the pitting characteristics of CCAs remain scarce. This includes studies that seek to understand the repassivation of CCAs. In any industrial application and context, the ability to repassivate following a corrosion event is critical. The complex chemistry of CCAs, including likely local chemistry alterations that would accompany localised dissolution and pitting, will have ramifications for repassivation. Such ramification may be either positive (beneficial) or negative, depending on local processes such as incongruent dissolution, dealloying or pit chemistry developed. Additionally, pitting characteristics of CCAs such as the number density, size and morphology of pits remain scarce. Such characteristics are the foundations of understanding microstructure–corrosion relationships for CCAs, which will require the combination of carefully controlled long-term exposures, and subsequent detailed microscopy.
- The surface chemistry of CCAs is largely unknown. Such a statement is broad, given that there exist (and we report) such a number of diverse types of CCA chemistries herein; however, the statement is universally applicable. A key question which remains to be addressed is the nature, composition and electronic/defect characteristics of the passive films formed upon a CCA surface. For example, many five element CCA with equiatomic proportions of elements have been reported; however, there is no general understanding of the surface film upon such alloys. For example, are such films comprises all the respective alloying elements, some alloying elements, the most reactive elements or only passivating elements? As one example, it is not clarified whether a Cr-based film forms upon Cr-containing CCAs or if the passive film itself is heterogeneous, comprising a mixture of different metallic oxides. Conversely, what is it that dictates the passivity in Cr-free CCAs? These questions may be capable of investigation using advanced characterisation techniques that including atom probe tomography with chemical composition measurements at the atomic scale, time-of-flight secondary ion mass spectrometry (TOF-SIMS) and XPS illuminating the origins of passivity in CCAs.
- Following on from the previous point, it is clear that many CCAs include significant variations in alloy chemistry over the microstructural length scales, from the nanoscale (such as shown in Fig. 1b), to the micrometre scale. Given the extent of associated elemental segregation, it remains unknown if such segregation leads to surface chemistry (i.e., passive film chemistry) variations over the multiphase surface. It would therefore be of significant value to investigate the corrosion of CCAs using 'local' electrochemical techniques such scanning electrochemical microscopy (SECM), the scanning vibrating electrode technique (SVET) and scanning Kelvin probe (SKP). Such local probe methods would enable one to monitor the influence of the heterogeneous microstructure on the corrosion of the CCAs, as revealing the distribution of anodes and cathodes at micrometre scale on the alloy surface. Quasi in situ scanning transmission electron microscopy of corroded specimens could provide valuable insights on the influence of nano-heterogeneities on alloy corrosion[78] and such an approach may be utilised for investigating the nano-scale corrosion of CCAs. The difficulty in deploying such methods will be in matching the technique with the length scales of interest, and factoring in the inherently slow corrosion rate of the most interesting CCAs. Methods such as online inductively coupled plasma-atomic emission spectroscopy tests (such as the AESEC technique reported by Ogle and co-workers[79]) could help quantify the incongruent dissolution rates of the different elements constituting the CCA.
- The industrial qualification of structural metals such as stainless steels and Al alloys requires extensive corrosion testing following any requisite standards. A structural alloy is usually typically tested for its resistance to atmospheric corrosion, pitting, crevice corrosion, intergranular corrosion, hydrogen embrittlement and stress corrosion cracking following standards such as the ASTM-G50 (practise for conducting atmospheric corrosion tests), ASTM-G48 (test of evaluating the pitting resistance of austenitic stainless steel), ASTM-A262 (for intergranular corrosion of stainless steel) etc. A similar matrix of tests for CCAs has not been presented and will be an important step in further highlighting the corrosion characteristics and for the qualification for any industrial applications.
- A systematic study on the corrosion of CoCrFeNi-based CCAs including $Al_xCoCrFeNi$, $CoCrFeNiCu_x$, $AlCoFeNiCr_x$, $CoCrFeNiTi_y$, $CoCrFeNiMo_x$ and $AlCoCrFeNi_x$ using rigorous electrochemical and surface characterisation could be explored as a first approach towards unravelling the corrosion characteristics of CCAs.

CONCLUSIONS

The corrosion characteristics of several CCAs were collated, reviewed and discussed herein. The nature of the literature to date makes it difficult to compare the corrosion performance of various HEAs/CCAs in detail, as each study has a unique focus, electrolyte and employs a specific analysis. Overall, the corrosion resistance of most CCAs are good, with their E_{corr}, E_{pit} and i_{corr} values being in the same range as austenitic and ferritic stainless

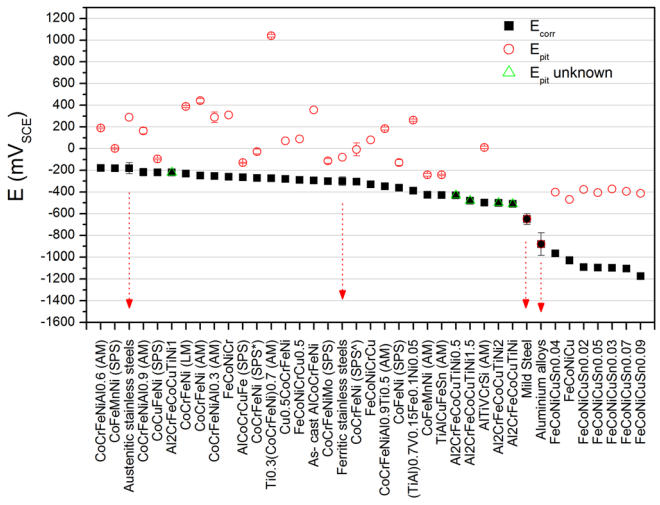

Fig. 16 A summary of the E_{corr} and E_{pit} values of different CCAs in quiescent 0.6 M NaCl at 25 °C. Here, LM denotes CCAs manufactured by laser melting (additive manufacturing/laser powder processing), AM denotes arc melting and SPS denotes spark plasma sintering. The alloy CoCrFeNi (SPS*) was produced by spark plasma sintering and held at 1000 °C for 5 min, while CoCrFeNi (SPS^) was firstly held at 500 °C for 5 min then sintered at 1000 °C for another 5 min. E_{corr} and E_{pit} value of CCAs are obtained from refs. 18, 48, 57, 58, 60, 69 The E_{corr} and E_{pit} data of steels and aluminium alloys are also presented for comparison.[25, 80, 81, 82, 83]

steels. What this indicates is that the general qualitative description of CRAs usually used to describe the families of stainless alloys, may be possibly extended to many CCAs. It is also an important point, in that the chemistry and heterogeneity of CCAs does not perhaps intuitively lead one to assume they will be CRAs.

The apparently good corrosion resistance of CCAs may be aided by most CCAs having Cr as one of their constituent (and often major) alloying elements (with >15 wt. % Cr). Therefore, the possibility of Cr-based passive film forming upon CCAs akin to that formed upon stainless steels is possible; however, the chemical composition of films upon CCAs remains largely unexplored to date. Similarly, the metallurgy (or the bulk CCA composition) required to achieve a specific surface film composition is wholly unexplored in the context of CCA alloy design for corrosion resistance. Advanced surface characterisation of CCAs needs to be performed to identify and ratify the chemical composition of their surface films. The oxide film formed upon CCAs may be comprising the most reactive (or least noble) element in the CCA, with noble metals dispersed into this film in either the oxidised or unoxidised states. From empirical results summarised herein, Mo and Ti are elements which serve to improve the corrosion resistance of CCAs. The presence of elements such as Al, Cu and B was shown to possibly compromise corrosion resistance, even in Cr-containing CCAs, but this was dependent on the overall CCA composition—and not general in all cases. The composition specific response is typified when looking at Al additions, in that the role of Al in undermining the passivity of CCAs is not clarified, although it is claimed that Al-rich regions in the CCA microstructure tend to become anodic with respect to Cr-rich regions; however, studies with variations in Al content have also shows a beneficial role for Al. These complex interactions, while frustrating a general understanding, reveal that optimisation of CCAs for corrosion resistance is both possible and unexplored. It has been reported that Cu tends to segregate in CCAs due to weak bonding between Cu and other elements, arising from a near zero or positive binary enthalpy of mixing. This results in the evolution of Cu-rich interdendrites and Cu-lean (and Cr-rich) dendrites in the microstructure of Cr and Cu-containing CCAs. To this end, selective dissolution of the Cu-rich interdendrites occurs has been demonstrated and evidence that localised corrosion can occur between these two compositionally distinct phases in a CCA.

The inferences on the corrosion behaviour of CCAs to date have been deduced essentially from so-called global methods, including immersion tests, potentiodynamic polarisation and EIS. The gaps and needs identified herein include the investigation of local electrochemical response via methods such as SECM, SVET or SKP.

The origin of passivity in CCAs is an important question which eludes the research community to date. This is not due to the understanding being complex or elusive per se, but due to the limited work and limited work focused on corrosion of HEAs/CCAs to date. Nonetheless, the corrosion resistance demonstrated thus far for CCAs is promising and undoubtedly CCAs may play several important roles in specific industrial applications. To this end, CCAs need to be tested specifically for the different forms of corrosion including atmospheric corrosion, pitting corrosion, crevice corrosion, intergranular corrosion, hydrogen-induced cracking and stress corrosion cracking. Standard procedures to test these forms of corrosion for CCAs therefore will need to either be adopted, or conceived and compiled.

Data availability

All relevant data are available from authors upon reasonable request.

ACKNOWLEDGEMENTS

The Australian Research Council is gratefully acknowledged for financial support. NB and ST are supported by Woodside Energy.

AUTHOR CONTRIBUTIONS

Yao Qiu, Sebastian Thomas, Mark Gibson, Hamish Fraser and Nick Birbilis reviewed and analysed the literature on the corrosion of high entropy alloys. Yao Qiu, Sebastian Thomas, Nick Birbilis wrote the paper. Mark Gibson and Hamish Fraser reviewed and modified the paper.

ADDITIONAL INFORMATION

Competing interests: The authors declare no competing financial interests.

Publisher's note: Springer Nature remains neutral with regard to jurisdictional claims in published maps and institutional affiliations.

REFERENCES

1. Yeh, J. W. et al. Nanostructured high-entropy alloys with multiple principal elements: novel alloy design concepts and outcomes. *Adv. Eng. Mater.* **6**, 299–303 (2004).
2. Cantor, B., Chang, I. T. H., Knight, P. & Vincent, A. J. B. Microstructural development in equiatomic multicomponent alloys. *Mater. Sci. Eng. A* **375-377**, 213–218 (2004).
3. Yeh, J. W. et al. Formation of simple crystal structures in Cu-Co-Ni-Cr-Al-Fe-Ti-V alloys with multiprincipal metallic elements. *Metall. Mater. Trans. A Phys. Metall. Mater. Sci.* **35A**, 2533–2536 (2004).
4. Qiu, Y. et al. A lightweight single-phase AlTiVCr compositionally complex alloy. *Acta Mater.* **123**, 115–124 (2017).
5. Jensen, J. K. et al. Characterization of the microstructure of the compositionally complex alloy $Al_1Mo_{0.5}Nb_1Ta_{0.5}Ti_1Zr_1$. *Scr. Mater.* **121**, 1–4 (2016).
6. Hsu, C. Y., Juan, C. C., Sheu, T. S., Chen, S. K. & Yeh, J. W. Effect of aluminum content on microstructure and mechanical properties of $Al_xCoCrFeMo_{0.5}Ni$ high-entropy alloys. *J. Metal* **65**, 1840–1847 (2013).
7. Shun, T. T., Chang, L. Y. & Shiu, M. H. Microstructures and mechanical properties of multiprincipal component CoCrFeNiTix alloys. *Mater. Sci. Eng. A* **556**, 170–174 (2012).
8. Zhang, Z. et al. Nanoscale origins of the damage tolerance of the high-entropy alloy CrMnFeCoNi. *Nat. Commun.* **6**, 10143 (2015).

9. Zou, Y., Ma, H. & Spolenak, R. Ultrastrong ductile and stable high-entropy alloys at small scales. *Nat. Commun.* **6**, 7748 (2015).
10. Gludovatz, B. et al. A fracture-resistant high-entropy alloy for cryogenic applications. *Science* **345**, 1153–1158 (2014).
11. Sriharitha, R., Murty, B. S. & Kottada, R. S. Alloying, thermal stability and strengthening in spark plasma sintered $Al_xCoCrCuFeNi$ high entropy alloys. *J. Alloy Compd.* **583**, 419–426 (2014).
12. Chuang, M. H., Tsai, M. H., Wang, W. R., Lin, S. J. & Yeh, J. W. Microstructure and wear behavior of $Al_xCo_{1.5}CrFeNi_{1.5}Ti_y$ high-entropy alloys. *Acta Mater.* **59**, 6308–6317 (2011).
13. Ma, S. G., Zhang, S. F., Gao, M. C., Liaw, P. K. & Zhang, Y. A Successful synthesis of the $CoCrFeNiAl_{0.3}$ single-crystal, high-entropy alloy by bridgman solidification. *J. Metal*, doi:10.1007/s11837-013-0733-x (2013).
14. Shun, T. T. & Du, Y. C. Microstructure and tensile behaviors of FCC $Al_{0.3}CoCrFeNi$ high entropy alloy. *J. Alloy Compd.* **479**, 157–160 (2009).
15. Sosa, J. M. et al. Three-dimensional characterisation of the microstructure of an high entropy alloy using STEM/HAADF tomography. *Mater. Sci. Technol.* **31**, 1250–1258 (2015).
16. Welk, B. A. et al. Nature of the interfaces between the constituent phases in the high entropy alloy CoCrCuFeNiAl. *Ultramicroscopy* **134**, 193–199 (2013).
17. Chen, Y. Y., Duval, T., Hung, U. D., Yeh, J. W. & Shih, H. C. Microstructure and electrochemical properties of high entropy alloys—a comparison with type-304 stainless steel. *Corros. Sci.* **47**, 2257–2279 (2005).
18. Qiu, Y., Gibson, M. A., Fraser, H. L. & Birbilis, N. Corrosion characteristics of high entropy alloys. *Mater. Sci. Technol.* **31**, 1235–1243 (2015).
19. He, J. Y. et al. Effects of Al addition on structural evolution and tensile properties of the FeCoNiCrMn high-entropy alloy system. *Acta Mater.* **62**, 105–113 (2014).
20. Wang, W.-R. et al. Effects of Al addition on the microstructure and mechanical property of $Al_xCoCrFeNi$ high-entropy alloys. *Intermetallics* **26**, 44–51 (2012).
21. Zhang, K. & Fu, Z. Effects of annealing treatment on phase composition and microstructure of $CoCrFeNiTiAl_x$ high-entropy alloys. *Intermetallics* **22**, 24–32 (2012).
22. Tang, Z. et al. Aluminum alloying effects on lattice types, microstructures, and mechanical behavior of high-entropy alloys systems. *J. Metal* **65**, 1848–1858 (2013).
23. Kao, Y. F., Chen, T. J., Chen, S. K. & Yeh, J. W. Microstructure and mechanical property of as-cast, -homogenized, and -deformed $Al_xCoCrFeNi$ ($0 \le x \le 2$) high-entropy alloys. *J. Alloy Compd.* **488**, 57–64 (2009).
24. Chou, H. P., Chang, Y. S., Chen, S. K. & Yeh, J. W. Microstructure, thermophysical and electrical properties in $Al_xCoCrFeNi$ ($0 \le x \le 2$) high-entropy alloys. *Mater. Sci. Eng. B* **163**, 184–189 (2009).
25. Jones, D. A. *Principle and Prevention of Corrosion* 2nd edn (Prentice-Hall, 1996).
26. Firouzdor, V., Sridharan, K., Cao, G., Anderson, M. & Allen, T. R. Corrosion of a stainless steel and nickel-based alloys in high temperature supercritical carbon dioxide environment. *Corros. Sci.* **69**, 281–291 (2013).
27. Lee, C. P., Chang, C. C., Chen, Y. Y., Yeh, J. W. & Shih, H. C. Effect of the aluminium content of $Al_xCrFe_{1.5}MnNi_{0.5}$ high-entropy alloys on the corrosion behaviour in aqueous environments. *Corros. Sci.* **50**, 2053–2060 (2008).
28. Kao, Y. F., Lee, T. D., Chen, S. K. & Chang, Y. S. Electrochemical passive properties of $Al_xCoCrFeNi$ (x = 0, 0.25, 0.50, 1.00) alloys in sulfuric acids. *Corros. Sci.* **52**, 1026–1034 (2010).
29. Li, B. Y. et al. Structure and properties of $FeCoNiCrCu_{0.5}Al_x$ high-entropy alloy. *Trans. Nonferrous Met. Soc. China* **23**, 735–741 (2013).
30. Mazzarolo, A., Curioni, M., Vicenzo, A., Skeldon, P. & Thompson, G. Anodic growth of titanium oxide: electrochemical behaviour and morphological evolution. *Electrochim. Acta* **75**, 288–295 (2012).
31. Scully, J. R. in Corrosion and Corrosion Prevention of Low Density Metals and Alloys: Proceedings of the International Symposium (eds Shaw, B. A., Buchheit, R. G. & Moran, J. P.) 187 (The Electrochemical Society, 2001).
32. Zhou, Y. J., Zhang, Y., Wang, Y. L. & Chen, G. L. Solid solution alloys of AlCoCrFeNiTi$_x$ with excellent room-temperature mechanical properties. *Appl. Phys. Lett.* **90**, 181904 (2007).
33. Wang, X. F., Zhang, Y., Qiao, Y. & Chen, G. L. Novel microstructure and properties of multicomponent $CoCrCuFeNiTi_x$ alloys. *Intermetallics* **15**, 357–362 (2007).
34. Ren, B., Zhao, R. F., Liu, Z. X., Guan, S. K. & Zhang, H. S. Microstructure and properties of $Al_{0.3}CrFe_{1.5}MnNi_{0.5}Ti_x$ and $Al_{0.3}CrFe_{1.5}MnNi_{0.5}Si_x$ high-entropy alloys. *Rare Metal* **33**, 149–154 (2014).
35. Choudhuri, D. et al. Formation of a Huesler-like L21 phase in a CoCrCuFeNiAlTi high-entropy alloy. *Scr. Mater.* **100**, 36–39 (2015).
36. Jiang, L. et al. Annealing effects on the microstructure and properties of bulk high-entropy $CoCrFeNiTi_{0.5}$ alloy casting ingot. *Intermetallics* **44**, 37–43 (2014).
37. Qiu, X. W., Zhang, Y. P. & Liu, C. G. Effect of Ti content on structure and properties of $Al_2CrFeNiCoCuTi_x$ high-entropy alloy coatings. *J. Alloy Compd.* **585**, 282–286 (2014).
38. Suter, T. & Böhni, H. Microelectrodes for studies of localized corrosion processes. *Electrochim. Acta* **43**, 2843–2849 (1998).
39. Birbilis, N. & Buchheit, R. Electrochemical characteristics of intermetallic phases in aluminum alloys an experimental survey and discussion. *J. Electrochem. Soc.* **152**, B140–B151 (2005).
40. Südholz, A. D., Kirkland, N. T., Buchheit, R. G. & Birbilis, N. Electrochemical properties of intermetallic phases and common impurity elements in magnesium alloys. *Electrochem. Solid State Lett.* **14**, C5 (2011).
41. Arjmand, F. & Adriaens, A. Microcapillary electrochemical droplet cells: applications in solid-state surface analysis. *J. Solid State Electrochem.* **18**, 1779–1788 (2014).
42. Sieradzki, K. & Newman, R. Percolation model for passivation in stainless steels. *J. Electrochem. Soc.* **133**, 1979–1980 (1986).
43. Shiobara, K., Sawada, Y. & Morioka, S. Potentiostatic study on the anodic behaviour of iron-chromium alloys. *Trans. Jpn. Inst. Metal* **6**, 58–62 (1965).
44. Newman, R., Meng, F. T. & Sieradzki, K. Validation of a percolation model for passivation of Fe-Cr alloys: I current efficiency in the incompletely passivated state. *Corros. Sci.* **28**, 523–527 (1988).
45. Asami, K., Hashimoto, K. & Shimodaira, S. An XPS study of the passivity of a series of iron—chromium alloys in sulphuric acid. *Corros. Sci.* **18**, 151–160 (1978).
46. Thomas, S., Birbilis, N., Venkatraman, M. S. & Cole, I. S. Self-repairing oxides to protect zinc: review, discussion and prospects. *Corros. Sci.* **69**, 11–22 (2013).
47. Chou, Y. L., Wang, Y. C., Yeh, J. W. & Shih, H. C. Pitting corrosion of the high-entropy alloy $Co_{1.5}CrFeNi_{1.5}Ti_{0.5}Mo_{0.1}$ in chloride-containing sulphate solutions. *Corros. Sci.* **52**, 3481–3491 (2010).
48. Li, Q. H., Yue, T. M., Guo, Z. N. & Lin, X. Microstructure and corrosion properties of AlCoCrFeNi high entropy alloy coatings deposited on AISI 1045 steel by the electrospark process. *Metall. Mater. Trans. A* **44**, 1767–1778 (2012).
49. Bhadeshia, H. K. D. H. & Honeycombe, S. R. in *Steels* 3rd edn (ed. H. K. D. H. BhadeshiaSir Robert Honeycombe) 259–286 (Butterworth-Heinemann, 2006)..
50. Newman, R. The dissolution and passivation kinetics of stainless alloys containing molybdenum—1. Coulometric studies of Fe-Cr and Fe-Cr-Mo alloys. *Corros. Sci.* **25**, 331–339 (1985).
51. Ilevbare, G. O. & Burstein, G. T. The inhibition of pitting corrosion of stainless steels by chromate and molybdate ions. *Corros. Sci.* **45**, 1545–1569 (2003).
52. Marshall, P. & Burstein, G. Effects of alloyed molybdenum on the kinetics of repassivation on austenitic stainless steels. *Corros. Sci.* **24**, 463–478 (1984).
53. Zhu, J. M. et al. Microstructures and compressive properties of multicomponent $AlCoCrFeNiMo_x$ alloys. *Mater. Sci. Eng. A* **527**, 6975–6979 (2010).
54. Chou, Y. L., Yeh, J. W. & Shih, H. C. The effect of molybdenum on the corrosion behaviour of the high-entropy alloys $Co_{1.5}CrFeNi_{1.5}Ti_{0.5}Mo_x$ in aqueous environments. *Corros. Sci.* **52**, 2571–2581 (2010).
55. Clayton, C. & Lu, Y. A bipolar model of the passivity of stainless steel: the role of Mo addition. *J. Electrochem. Soc.* **133**, 2465–2473 (1986).
56. Crook, P. Corrosion resistance Nickel alloys Part 1. *Adv. Mater. Process* **165**, 37–39 (2007).
57. Qiu, X. W. & Liu, C. G. Microstructure and properties of $Al_2CrFeCoCuTiNi_x$ high-entropy alloys prepared by laser cladding. *J. Alloy Compd.* **553**, 216–220 (2013).
58. Hsu, Y. J., Chiang, W. C. & Wu, J. K. Corrosion behavior of $FeCoNiCrCu_x$ high-entropy alloys in 3.5% sodium chloride solution. *Mater. Chem. Phys.* **92**, 112–117 (2005).
59. Ren, B. et al. Corrosion behavior of CuCrFeNiMn high entropy alloy system in 1 M sulfuric acid solution. *Mater Corrosion*. **63**, 828–834 (2011).
60. Lin, C.-M., Tsai, H.-L. & Bor, H.-Y. Effect of aging treatment on microstructure and properties of high-entropy $Cu_{0.5}CoCrFeNi$ alloy. *Intermetallics* **18**, 1244–1250 (2010).
61. Hemphill, M. A. et al. Fatigue behavior of $Al_{0.5}CoCrCuFeNi$ high entropy alloys. *Acta Mater.* **60**, 5723–5734 (2012).
62. Tong, C. J. et al. Microstructure characterization of $Al_xCoCrCuFeNi$ high-entropy alloy system with multiprincipal elements. *Metall. Mater. Trans. A Phys. Metall. Mater. Sci.* **36A**, 881–893 (2005).
63. Tsai, C. W., Tsai, M. H., Yeh, J. W. & Yang, C. C. Effect of temperature on mechanical properties of Al0.5CoCrCuFeNi wrought alloy. *J. Alloy. Compd.* **490**, 160–165 (2010).
64. Hsu, C. Y., Yeh, J. W., Chen, S. K. & Shun, T. T. Wear resistance and high-temperature compression strength of Fcc $CuCoNiCrAl_{0.5}Fe$ alloy with boron addition. *Metall. Mater. Trans. A* **35**, 1465–1469 (2004).
65. Lee, C. P., Chen, Y. Y., Hsu, C. Y., Yeh, J. W. & Shih, H. C. The effect of boron on the corrosion resistance of the high entropy alloys $Al_{0.5}CoCrCuFeNiB_x$. *J. Electrochem. Soc.* **154**, C424–C430 (2007).
66. Zhang, C., Chen, G. J. & Dai, P. Q. Evolution of the microstructure and properties of laser-clad $FeCrNiCoB_x$ high-entropy alloy coatings. *Mater Sci Technol.* **32**, 1–7 (2016).

67. Liu, L., Zhu, J. B., Zhang, C., Li, J. C. & Jiang, Q. Microstructure and the properties of $FeCoCuNiSn_x$ high entropy alloys. *Mater. Sci. Eng. A* **548**, 64–68 (2012).
68. Sun, Z. Y., Zhang, J., Zhu, J. B. & Li, J. C. Microstructure and the properties of $AlFeCoNiCrSn_x$ high-entropy alloys. *Arab. J. Sci. Eng.* **39**, 8247–8251 (2014).
69. Zheng, Z. Y., Li, X. C., Zhang, C. & Li, J. C. Microstructure and corrosion behaviour of $FeCoNiCuSn_x$ high entropy alloys. *Mater. Sci. Technol.* **31**, 1148–1152 (2014).
70. Lee, C. P., Chen, Y. Y., Hsu, C. Y., Yeh, J. W. & Shih, H. C. Enhancing pitting corrosion resistance of $Al_xCrFe_{1.5}MnNi_{0.5}$ high-entropy alloys by anodic treatment in sulfuric acid. *Thin Solid Films* **517**, 1301–1305 (2008).
71. Siddiqui, R. A., Abdullah, H. A. & Al-Belushi, K. R. Influence of aging parameters on the mechanical properties of 6063 aluminium alloy. *J. Mater. Process Technol.* **102**, 234–240 (2000).
72. Beldjoudi, T., Fiaud, C. & Robbiola, L. Influence of Homogenization and artificial aging heat treatments on corrosion behavior of Mg-Al alloys. *Corrosion* **49**, 738–745 (1993).
73. Lin, C. M. & Tsai, H. L. Evolution of microstructure, hardness, and corrosion properties of high-entropy $Al_{0.5}CoCrFeNi$ alloy. *Intermetallics* **19**, 288–294 (2011).
74. Zhang, C., Zhang, F., Chen, S. & Cao, W. Computational thermodynamics aided high-entropy alloy design. *J. Metal* **64**, 839–845 (2012).
75. Hsu, C. Y. et al. Phase diagrams of high-entropy alloy system Al-Co-Cr-Fe-Mo-Ni. *J. Metal* **65**, 1829–1839 (2013).
76. Zhang, F. et al. An understanding of high entropy alloys from phase diagram calculations. *Calphad* **45**, 1–10 (2014).
77. Gupta, R. K. et al. Simultaneous improvement in the strength and corrosion resistance of Al via high-energy ball milling and Cr alloying. *Mater. Des.* **84**, 270–276 (2015).
78. Qiu, X. W. Microstructure and properties of AlCrFeNiCoCu high entropy alloy prepared by powder metallurgy. *J. Alloy Compd.* **555**, 246–249 (2013).
79. Cheng, J. B., Liang, X. B. & Xu, B. S. Effect of Nb addition on the structure and mechanical behaviors of CoCrCuFeNi high-entropy alloy coatings. *Surf. Coat. Technol.* **240**, 184–190 (2014).
80. Sedriks, A. J. *Corrosion of Stainless Steels* 2nd edn (Wiley-Interscience, 2006).
81. Davis, J. R. *Corrosion of Aluminum and Aluminum Alloys* (ASM International, 1999).
82. Kairy, S. K., Rometsch, P. A., Davies, C. H. J. & Birbilis, N. On the electrochemical and quasi in situ corrosion response of the Q-Phase ($Al_xCu_yMg_zSiw$) intermetallic particle in 6xxx series aluminium alloys. *Corrosion* **73**, 87–99 (2016).
83. Ogle, K. Atomic emission spectroelectrochemistry: a new look at the corrosion, dissolution and passivation of complex materials. *Corros. Mater.* **37**, 60–67 (2012).